Scuola di Dottorato in Ingegneria Leonardo da Vinci – a.a. 2009/10

PROPRIETÀ MECCANICHE, OTTICHE, ELETTRONICHE DEI MATERIALI ALLE PICCOLE E PICCOLISSIME SCALE

Versione 1 – Settembre 2010 – http://www.df.unipi.it/~fuso/dida

Parte 4
Proprietà meccaniche a scala nanometrica: microscopia a scansione di forza (AFM)

Ve 24.09 15-16 aula 6 DCCI
Me 29.09 13-15 aula DF

Outlook

- General features of Scanning Probe Microscopy
- Forces at the small and ultra-small scales: repulsive and attractive charatcer (contact, non-contact)
- Using the force at the small and ultra-small scales to imgae samples with unprecedented resolution:
  the Atomic Force Microscopy (AFM) and its variants
- *(to be discussed in the next seminars: how to use AFMs to measure mechanical properties at the nanoscale)*

Basics of Scanning Probe Microscopy (SPM)

Scanning: piezoelectric translator
Probe: tip probing local properties
Microscopy: sub-micrometer resolution
(+ system to control tip/sample distance
+ electronics for instrument operation)

Developed starting since '80s thanks to:

✓Piezo translators with sub-nm resolution;
✓sub-nm probes

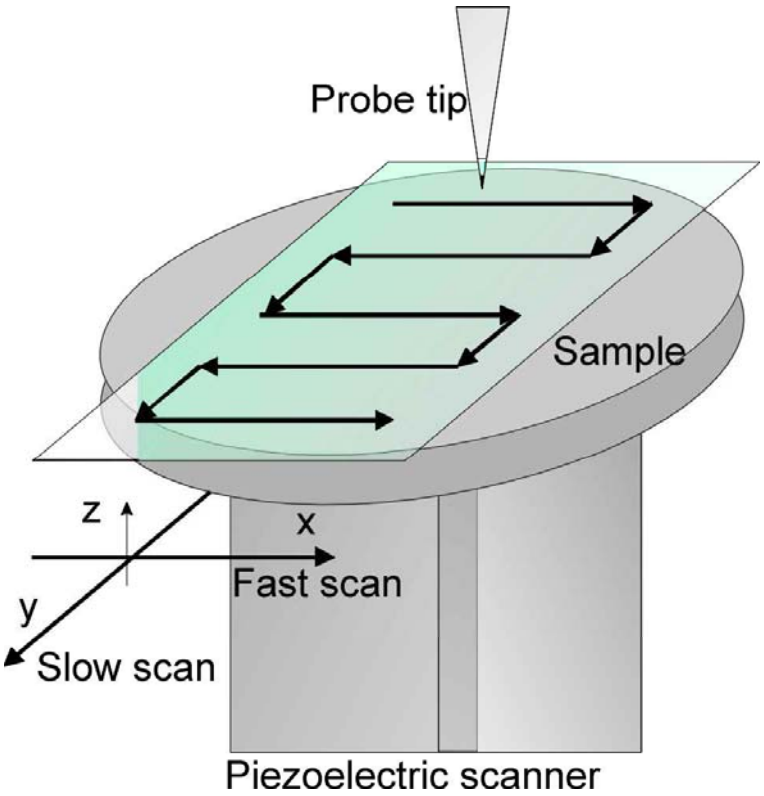

Various physical quantities can be measured point-by-point during the scan and an image (i.e., a map of the quantity) can be built up

A few examples of SPMs

	Technique	Probed quantity	Resolution
	STM	Electron tunneling	atomic
SFM	AFM	Mechanical force	1 nm
SFM	SFFM	Friction force	
SFM	MFM	Local magnetization	10 nm
SFM	EFM	Local polarization	
	SNOM	Optical properties	
	Ap-SNOM	Optical properties	50 nm
	...	...	

Depending on the probe and on its interaction with the surface, a variety of physical effects can be investigated

A few preliminary considerations on scans

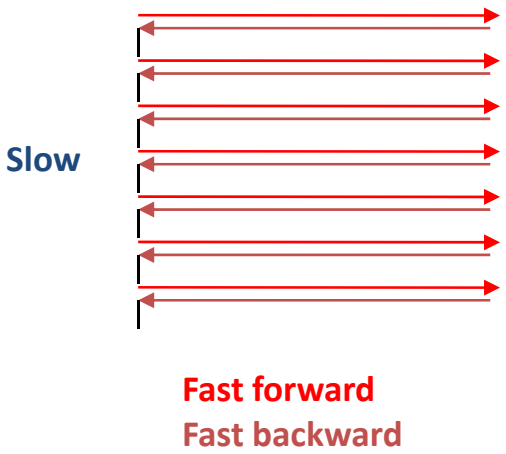

Normally, a **raster scan** is applied:

- Scan addresses an array of discrete, equispaced "pixels" (e.g., 64x64, 128x128, 256x256,…);
- Scan speed is different for one and the other directions (**fast and slow** scans, respectively);
- **Forward** (trace) and **backward** (retrace) scans along the "fast axis" are typically acquired;
- Forward/backward **comparison** is routinely used to assess the scan quality (unless it is used to derive some physical quantity, as in LFM)

The acquisition speeds depends on:
- Time response of the scanner (typically a few ms for nm-sized displacements);
- The signal-to-noise of the quantity to be probed and acquired (through μs to s depending on the nature of the measurement)

Rule of thumb: fast acquisition are more suited to higher resolution (in order to prevent thermal and mechanical drifts)

A few details: piezoelectric scanner

[illegible] coefficient d is negative representing contraction perpendicular to the field; and positive for stain measured along the 3-direction (along which the thickness t is measured) representing expansion parallel to the electric field direction:

$$\Delta t = d_{33} V . \qquad (4.4)$$

Although there are many ceramic compositions used today, most can be placed into two general categories: hard and soft PZT materials. Typical d coefficients for hard PZT materials are

$$d_{33} = 250 \cdot 10^{-12}\ \mathrm{m/V}, \quad d_{31} = -110 \cdot 10^{-12}\ \mathrm{m/V};$$

and for soft PZT materials

$$d_{33} = 600 \cdot 10^{-12}\ \mathrm{m/V}, \quad d_{31} = -270 \cdot 10^{-12}\ \mathrm{m/V}.$$

For PZT-5H

$$d_{33} = 593 \cdot 10^{-12}\ \mathrm{m/V}, \quad d_{31} = -273 \cdot 10^{-12}\ \mathrm{m/V}.$$

Typ: hollow tubes made of PZT-based ceramics with a multi-electrode configuration aimed at controlling the displacement along different directions.

Main issues:
- Linearity (possibly closed loop);
- Hysteresis;
- Distorted motion (*artifacts*).

Displacement as small as ~ 0.1-0.5 nm/V (along Z) are possible

Typical "scanner sensitivity":
~1-10 nm/V (along Z)
~1-100 nm/V (along XY)

Typical driving voltages up to ±250 V

Typical min driving step size (16 bit) ~10 mV

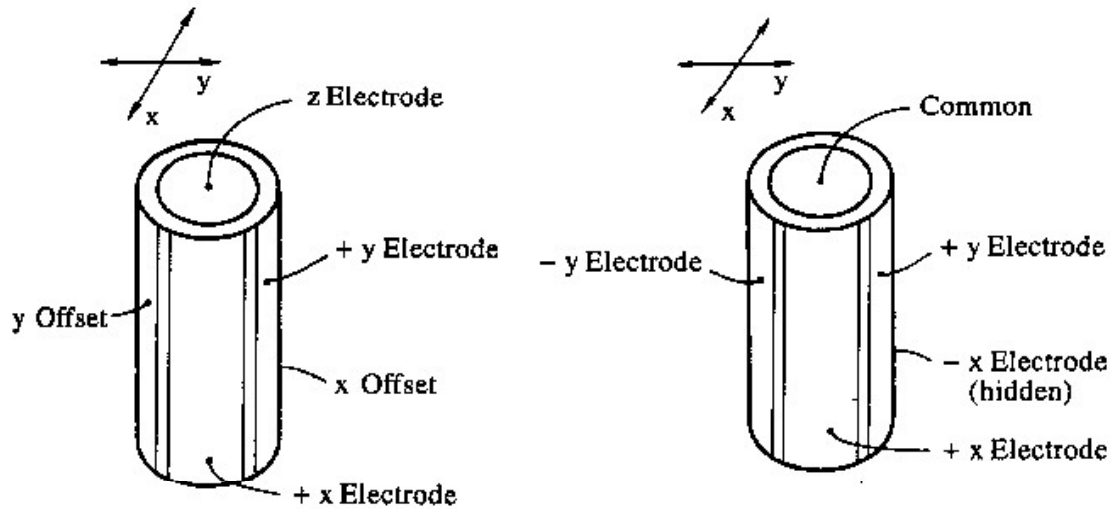

Fig. 4.5. Illustrating the voltages applied to the electrodes of the single-tube scanner

Da C. Bai, STM and its applications (Springer, 1995)

Scanner-related artifacts I

Artifacts mean the presence of spurious information in an SPM image
The easiest way to approach the artifact problem is in AFM (we'll see soon how it works!)

2.0 Scanner Artifacts

Scanners that move the probe in an atomic force microscope in the X, Y and Z directions are typically made from piezoelectric ceramics. As electromechanical transducers, piezoelectric ceramics are capable of moving a probe very small distances. However, when a linear voltage ramp is applied to piezoelectric ceramics, the ceramics move in a nonlinear motion. Further, the piezoelectric ceramics exhibit hysteresis effects caused by self-heating. Artifacts can also be introduced into images because of the geometry of the scanner. The positioning of the scanner relative to the sample can also create artifacts.

2.2. X-Y Calibration/Linearity

All atomic force microscopes must be calibrated in the X-Y axis so that the images presented on the computer screen are accurate. Also the motion of the scanners must be linear so that the distances measured from the images are accurate. With no correction, the features on an image will typically appear smaller on one side of the image than on the other.

2.6. Scanner Drift

Drift in AFM images can occur because of thermal drift in the piezoelectric scanner and because an AFM can be susceptible to external temperature changes. The most common type of drift occurs at the beginning of a scan of a zoomed-in region of an image. This artifact causes the initial part of a scan range to appear distorted. Drift artifacts are most easily observed when imaging test patterns. Drift will cause lines that should appear straight to have curvature.

Figure 16

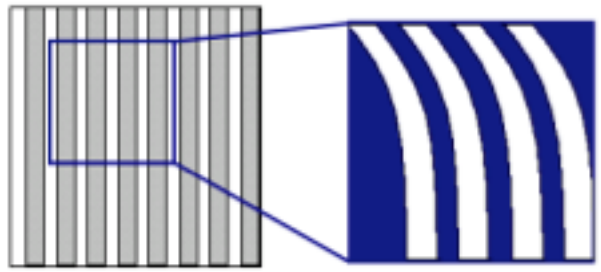

After a region of a sample is scanned with the AFM it is common to "zoom" into a small section of the image to get a higher magnification of an image. Scanner drift will cause the image to appear distorted at the beginning of the scan.

Figure 17

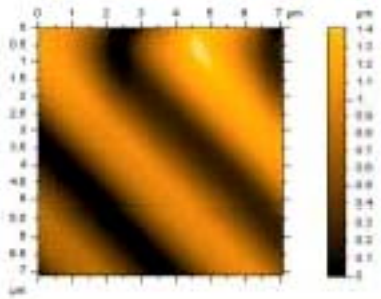

Zoomed image showing a distortion at the beginning of the scan. The scan angle is 45 degrees.

Scanner-related artifacts II

2.4. Background Bow/Tilt

The piezoelectric scanners that move the probe in an atomic force microscope typically move the probe in a curved motion over the surface. The curved motion results in a "Bow" in the AFM image. Also, a large planar background or "Tilt" can be observed if the probe/sample angle is not perpendicular.

Often the images measured by the AFM include a background "Bow" and a background "Tilt" that are larger than the features of interest. In such cases the background must be subtracted from the image. This is often called "leveling" or "flattening" the image. After "leveling" the desired features are typically directly seen in the image.

Figure 12

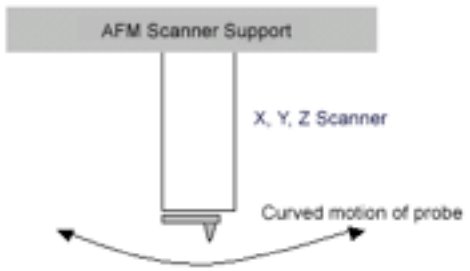

An AFM piezoelectric scanner is often supported at the top by a mechanical assembly. Thus the motion of the probe is nonlinear in the Z axis as it is scanned across a surface. The motion can be spherical or even parabolic depending on the type of piezoelectric scanner.

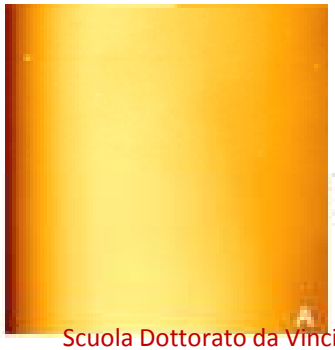

Figure 13A-B: Image (A) is an 85 X 85 micron image of a flat piece of silicon. The bow introduced into the image is seen at the edges. (B) A line profile across this image shows the magnitude of the bow.

(Image) post-processing can help
(but may introduce new artifacts, as well…)

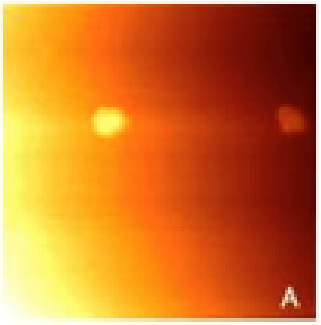

Figure 21A-C: AFM images a 1.6 X 1.6 micron image of nanospheres on a surface.

(A) The original image measured by the AFM before any image processing. Tilt is easily recognized in the image as the right side of the image appears darker than the left side of the image.

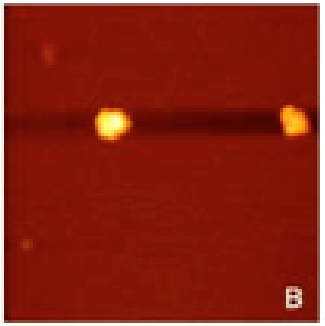

(B) The AFM image shown in "A" after a line-by-line leveling of the image with a first order background correction. The dark band in the image is caused by the image processing and is not a real structure.

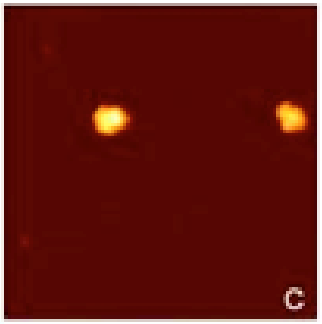

(C) Particles are excluded from the background subtraction process to derive this image.

Closed-loop scanners

- ✓ Problems associated with the scanner geometry can be solved by using different scanner configurations (e.g., non cylindrical)
- ✓ Problems associated with non-linearity, hysteresis, drifts, can be solved by using closed-loop scanners (displacement is indipendently measured, e.g., by capacitive or interferometric or resistive means, and a loop is applied)

PI

Excellent performances presently achievable

Nanometer Accuracy in 1 millisecond with 50-picometer Resolution
PicoCube® systems provide resolution of 50 picometers and below. The ultra-fast XY/XYZ piezo drives offer resonant frequencies of 9.8 kHz in Z and >3 kHz in X and Y! The high resonant frequency and high-bandwidth capacitive feedback allow step and settle to 1% accuracy in as little as one millisecond.

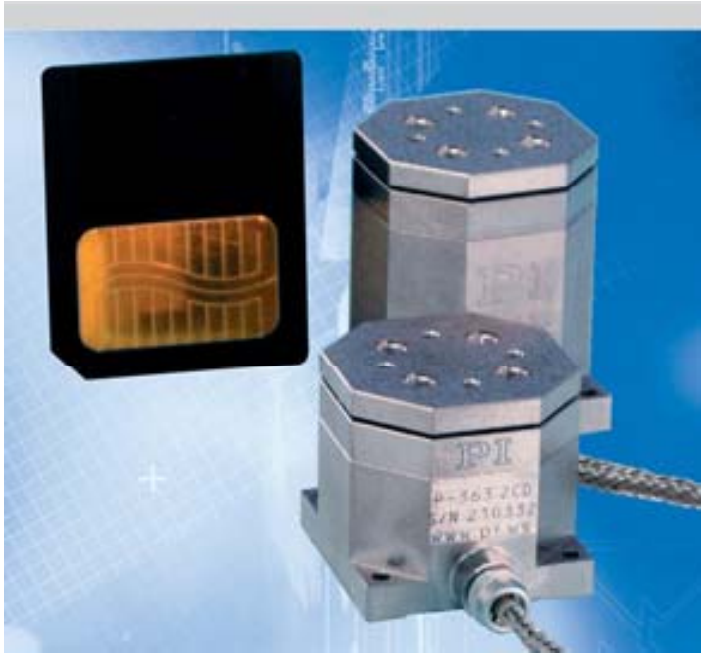

2. Scanning force microscopy (AFM and relatives)

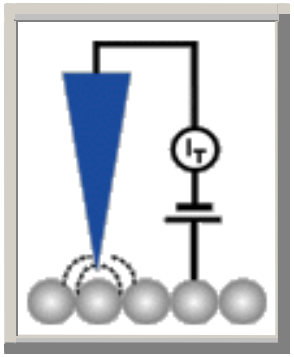	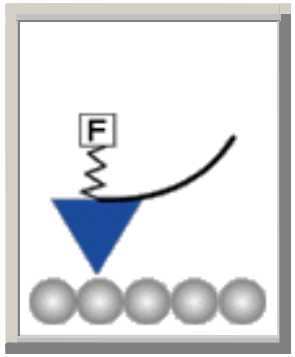	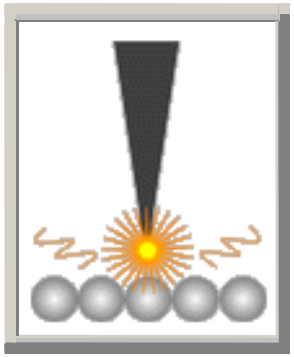
STM **Electron tunneling**	AFM **Force microscopy** **Locally probed quantity**	SNOM **Optical near-field**

AFM is probably the most straightforward (and easy to understand/interpret) probe microscopy (and, for sure, the one with the largest worldwide diffusion)

AFM probes

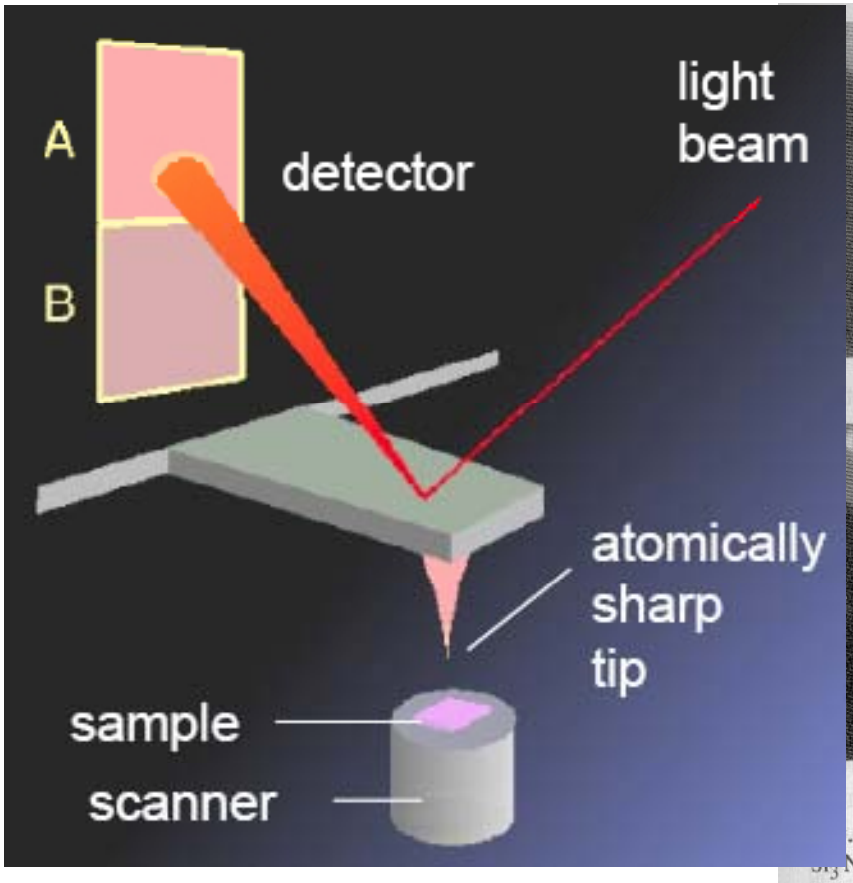

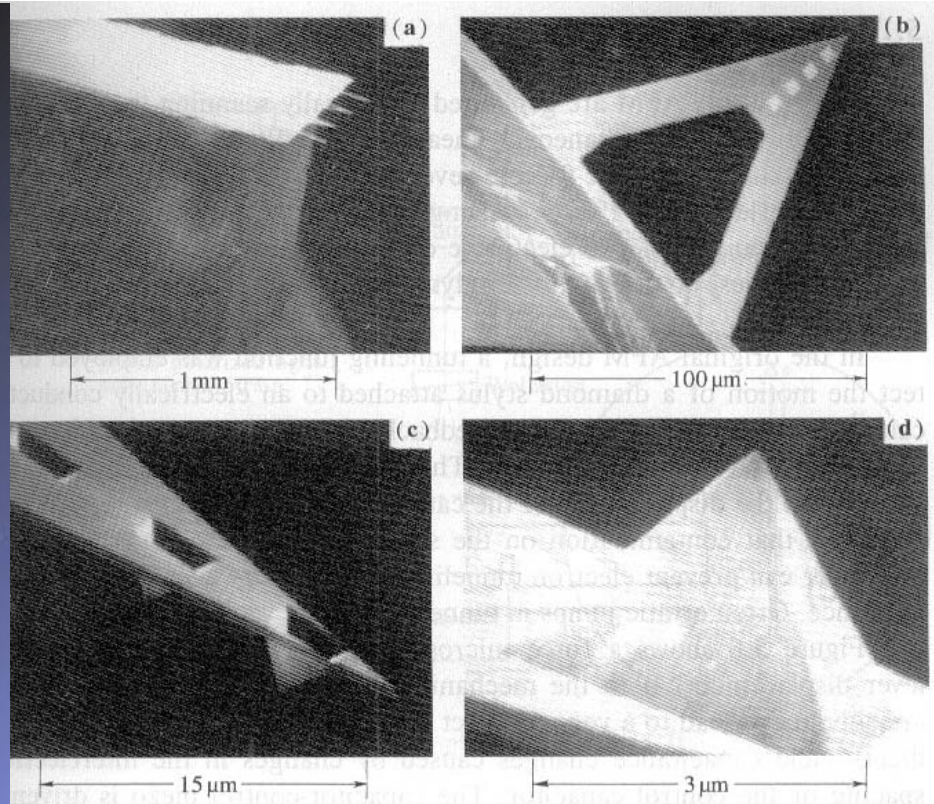

. 5.5a-d. SEM micrographs of Si_3N_4 cantilevers with integrated pyramidal tips. (**a**) The Si_3N_4 film is attached to the surface of a glass block with dimensions of $2 \times 3 \times 0.7$ mm^3. Four cantilevers protrude from the edge of the block. (**b**) Four pyramidal tips can be seen at the end of this V-shaped cantilever. (**c**) The pyramidal tips are hollow when viewed from the back side. (**d**) Each tip has very smooth sidewalls, and the tip appears to terminate virtually at a point, with less than 30 nm radius [5.4]

The local character of AFM relies on the availability of suitable probes

Microfabricated cantilevers

Cantilevered beams are the most ubiquitous structures in the field of microelectromechanical systems (MEMS). An early example of a MEMS cantilever is the Resonistor[4][5], an electromechanical monolithic resonator. MEMS cantilevers are commonly fabricated from silicon (Si), silicon nitride (SiN), or polymers. The fabrication process typically involves undercutting the cantilever structure to *release* it, often with an anisotropic wet or dry etching technique. Without cantilever transducers, atomic force microscopy would not be possible. A large number of research groups are attempting to develop cantilever arrays as biosensors for medical diagnostic applications. MEMS cantilevers are also finding application as radio frequency filters and resonators. The MEMS cantilevers are commonly made as unimorphs or bimorphs.

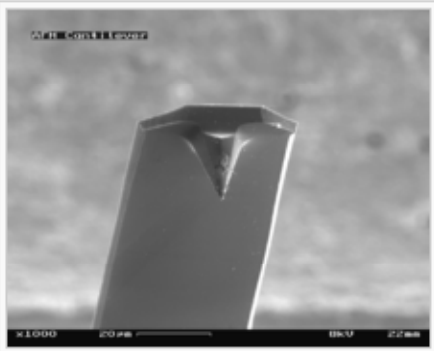

SEM image of a used AFM cantilever

Two equations are key to understanding the behavior of MEMS cantilevers. The first is *Stoney's formula*, which relates cantilever end deflection δ to applied stress σ:

$$\delta = \frac{3\sigma\left(1-\nu\right)}{E}\left(\frac{L}{t}\right)^2$$

where v is Poisson's ratio, E is Young's modulus, L is the beam length and t is the cantilever thickness. Very sensitive optical and capacitive methods have been developed to measure changes in the static deflection of cantilever beams used in dc-coupled sensors.

The second is the formula relating the cantilever spring constant k to the cantilever dimensions and material constants:

$$k = \frac{F}{\delta} = \frac{Ewt^3}{4L^3}$$

where F is force and w is the cantilever width. The spring constant is related to the cantilever resonance frequency ω_0 by the usual harmonic oscillator formula $\omega_0 = \sqrt{k/m}$. A change in the force applied to a cantilever can shift the resonance frequency. The frequency shift can be measured with exquisite accuracy using heterodyne techniques and is the basis of ac-coupled cantilever sensors.

The principal advantage of MEMS cantilevers is their cheapness and ease of fabrication in large arrays. The challenge for their practical application lies in the square and cubic dependences of cantilever performance specifications on dimensions. These superlinear dependences mean that cantilevers are quite sensitive to variation in process parameters. Controlling residual stress can also be difficult.

Cantilever/tip fabrication: examples

The first step in the fabrication of an AFM tip is the etching of a single-crystal silicon wafer with specific crystalline orientation. This results in the forming of square pyramidal tips with characteristic angles.

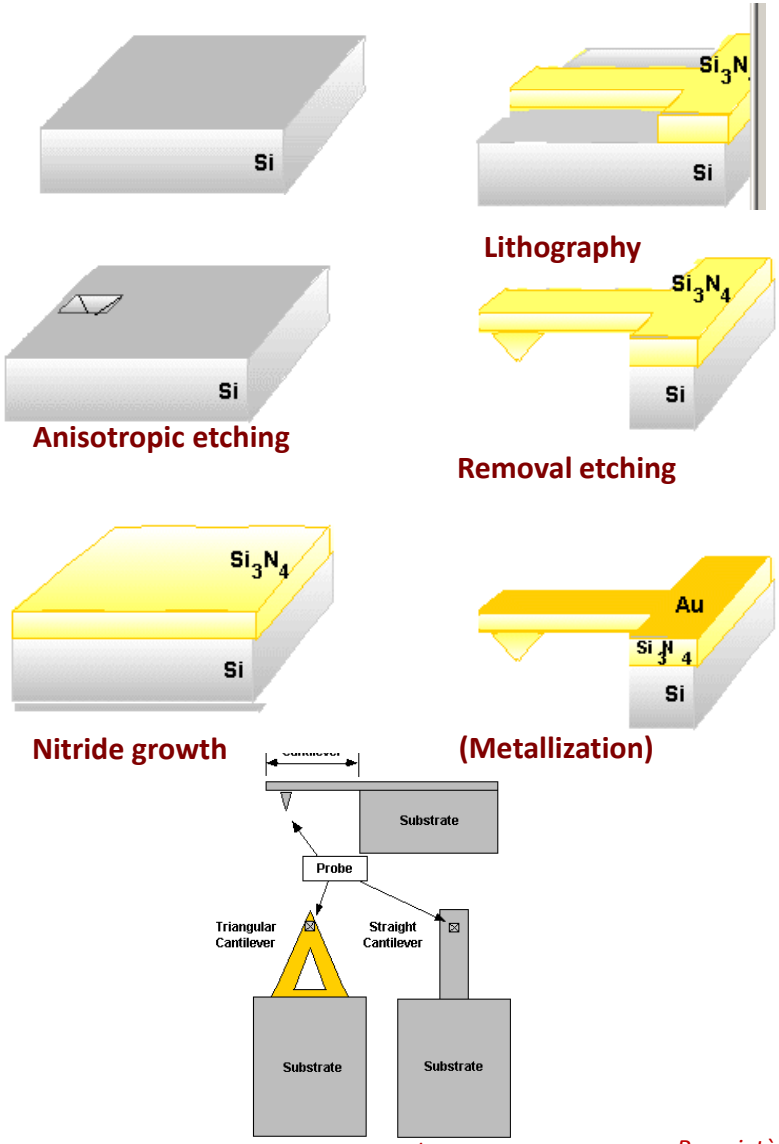

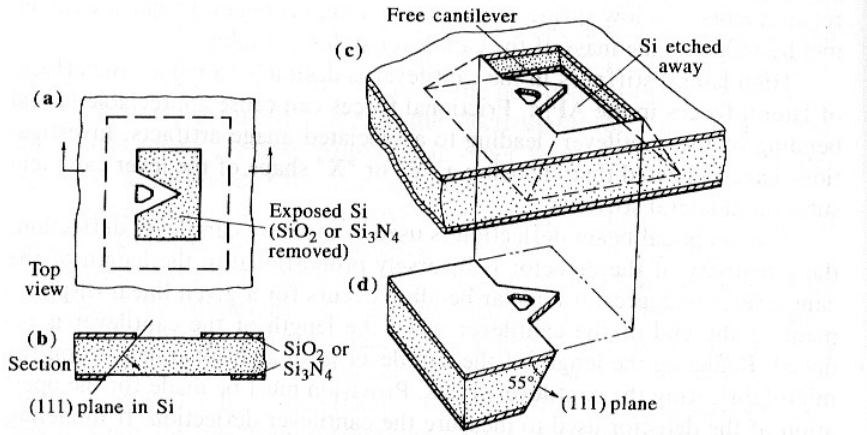

Fig. 5.2a-d. Fabrication of thin-film microcantilevers. (**a**) A thin film of SiO_2 or Si_3N_4 is formed on the surface of a (100) Si wafer and patterned to define the shape of the cantilever and to create openings on the top and bottom of the wafer. (**b**) The windows are aligned along (111) planes. (**c**) Anisotropic etching of the exposed Si with KOH undercuts the cantilever and self-terminates at the (111) planes as shown. (**d**) A small Si chip is cut from the wafer to serve as a pedestal for mounting the cantilever in the AFM [5.4]

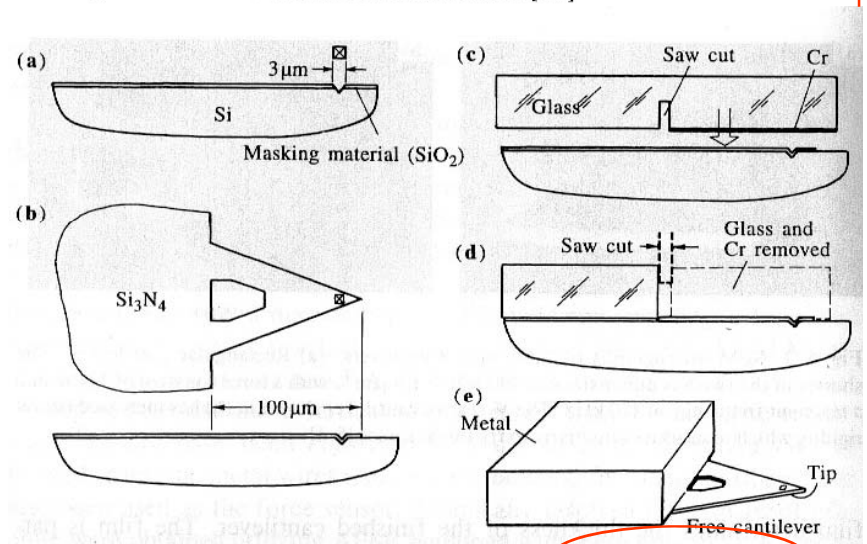

Fig. 5.4a-e. Fabrication of Si_3N_4 microcantilevers with integrated pyramidal tips (**a**) to (**c**) illustrate the steps in the fabrication process, see text [5.4]

Examples of commercial cantilevers

FEATURES:

- Compatible with all major AFM brands.
- Typical radius of curvature: sharpened tips: < 20 nm., unsharpened tips: < 50 nm.
- Available with gold coating for high reflectivity.
- Recessed corners for easy sample approach.
- The widest range of spring constants commercially available on a single chip.

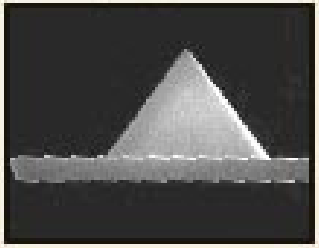

ThermoMicroscopes Microlevers are ideal for all contact imaging modes, force modulation microscopy, and liquid operation. The range in force constants enable users to image soft samples in contact as well as high load force vs. distance spectroscopy.

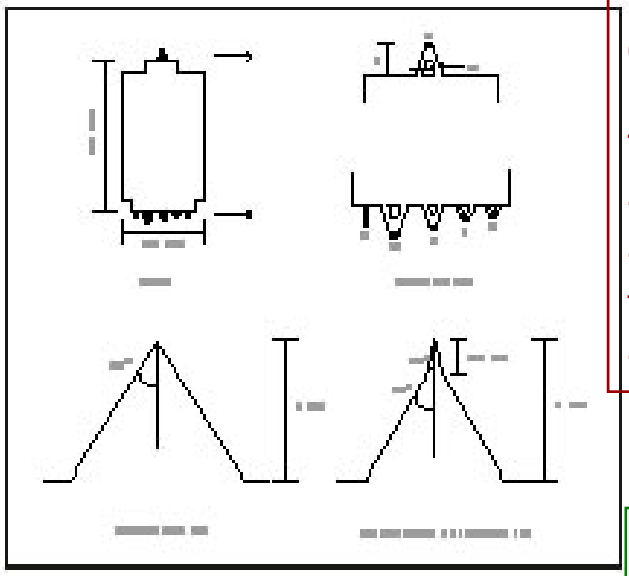

Many different cantilevers are commercially available

They are different for:
-Dimensions and shape, typ 0.1-0.5 mm:
-Elastic constant (materials and design, typ 0.05-50 N/m;
-Tip coating (conductive, super-hard, etc.)

Typical Mechanical Characteristics

Cantilever type	A - triangular	B - rectangular	C - triangular	D - triangular	E - triangular	F - triangular
Standard mode of operation	Contact					
Cantilever length	180 µm	200 µm	320 µm	220 µm	140 µm	85 µm
Cantilever width	18 µm	20 µm	22 µm	22 µm	18 µm	18 µm
Cantilever thickness	0.6 µm	0.6 µm	0.6 µm	0.6 µm	0.6 µm	0.6 µm
Force Constant	0.05 N/m	0.02 N/m	0.01 N/m	0.03 N/m	0.10 N/m	0.50 N/m
Resonant Frequency	22 kHz	15 kHz	7 kHz	15 kHz	38 kHz	120 kHz

Ordering Information

Microlevers	Sharpened		Unsharpened	
Quantity	Gold coated*	Uncoated	Gold coated*	Uncoated
Half wafer - (250 chips)	MSCT-AUHW	MSCT-NOHW	MLCT-AUHW	MLCT-NOHW
Unmounted - (25 chips)	MSCT-AUNM	MSCT-NONM	MLCT-AUNM	MLCT-NONM
Mounted - (25 chips)	MSCT-AUMT-A	MSCT-NOMT-A	MLCT-AUMT-A	MLCT-NOMT-A
Mounted - (25 chips)	MSCT-AUMT-BF	MSCT		F

* Not for use with AutoProbe M5 systems

THERMOMICROSCOPES

Microlevers™

GENERAL PURPOSE CANTILEVERS

Cantilever choice depends for instance on:
-Operation mode (contact/non contact);
-Quantities to be probed (e.g., if an electric field is needed, a conductive tip has to be used);
-Possible material manipulation (e.g., nanoindentation requires super-hard tips)

Basics of tip/sample interaction

When the tip is approached to the sample (at sub-nm distance!), forces depend roughly on van der Waals interaction (see Lennard-Jones) between apical tip atoms and surface

At "large" distance forces are weakly attractive, at "short" distance they are repulsive

Surface topography (height variations) can be sensed by monitoring the force, i.e., the **cantilever deflection**

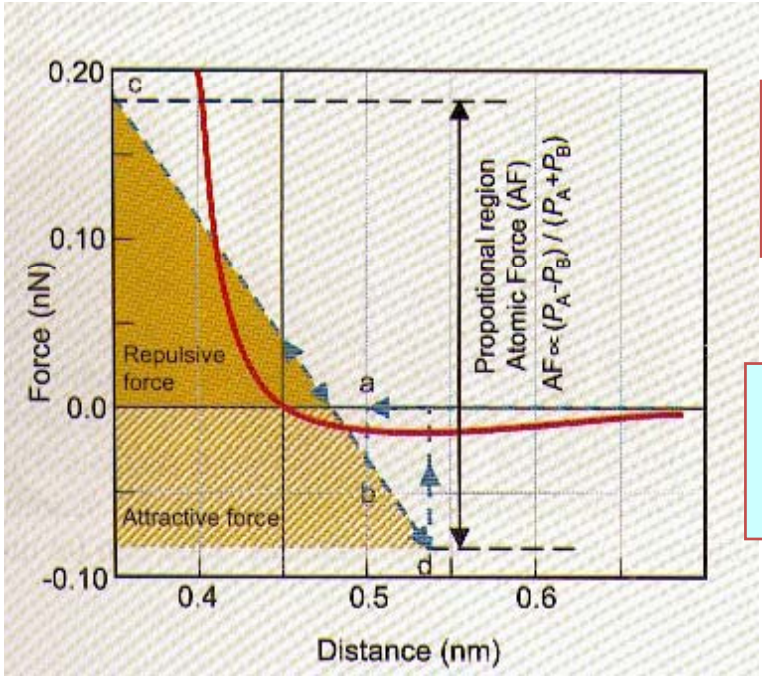

When tip/sample distance is kept in the repulsive region, **contact operating mode** is achieved

When tip/sample distance is kept *(mostly)* in the attractive region, **non-contact operating mode** is achieved

Tip/sample forces

Sample investigation is available thanks to the forces acting between a cantilever and a surface. They are quite different. One or another force dominate at different tip-sample separations.

- During contact and the surface deformation by the cantilever, the elastic repulsion force dominates; this approximation is called the **Hertz model** and is considered in the chapter "Elastic interactions. The Hertz problem".
- At tip-sample separations of the order of several tens of angstrom the major interaction is the intermolecular interaction called the **Van der Waals force** (see chapter "The Van der Waals force").
- At the same distance between the tip and the sample and in the presence of liquid films, the interaction is influenced much by **capillary and adhesion forces**. The range of capillary forces considered in the chapter "Capillary forces" is determined by the liquid film thickness.
- At larger separations the **electrostatic interaction** starts to dominate. It is described in chapter "Electrostatic force microscopy".
- At separations of the order of a thousand of angstroms **magnetic forces** considered in the chapter "Magnetic force microscopy" prevail.

Various kind of forces do cooperate in providing the typical force vs distance behavior experienced in AFM

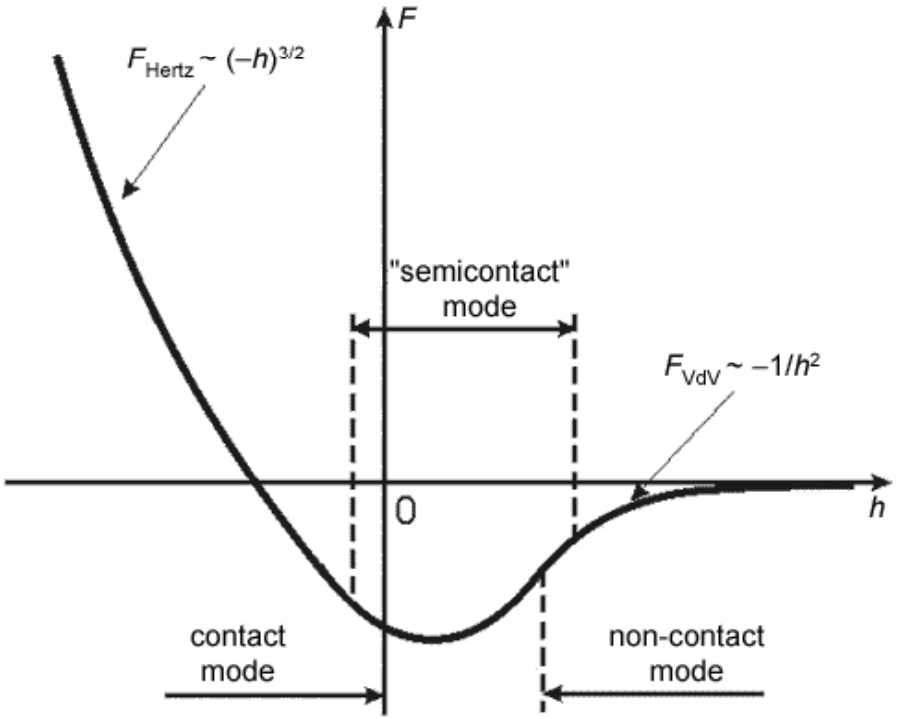

A few words on van der Waals I

The Van der Waals force or the intermolecular attractive force has three components of slightly different physical nature but having the same potential dependence on the intermolecular distance – $1/r^6$. This lucky circumstance allows to compare directly constants of interaction that correspond to three Van der Waals force components because proportions between them will be held constant at different r magnitudes. Constants at $1/r^6$ multiplier will differ for various materials.

$$W = W_{\text{orient}} + W_{\text{ind}} + W_{\text{disp}} \sim 1/r^6 \qquad (1)$$

All three Van der Waals force components are based on dipoles interaction, therefore we should remember two basic formulas:

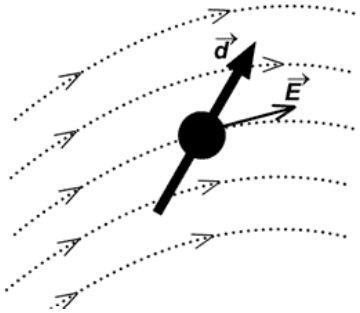

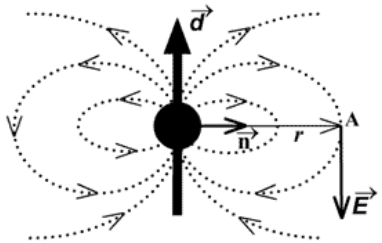

the energy of dipole $\mathbf{d}$ placed in field $\mathbf{E}$ is [1]:

$$W_D = -\mathbf{dE} \qquad (2)$$

and the electric field produced by the dipole $\mathbf{d}$ is [1]:

$$\mathbf{E} = \frac{\left(3(\mathbf{nd})\mathbf{n} - \mathbf{d}\right)}{r^3}, \quad |\mathbf{E}| \sim \frac{1}{r^3} \qquad (3)$$

where $\mathbf{n}$ – unit vector directed from the point at which the energy is determined to the dipole.

The orientational interaction (or the **Casimir force**) arises between two polar molecules each of which has the electric dipole moment. In accordance with (2), (3) the interaction energy of dipoles $\mathbf{d}_1$ and $\mathbf{d}_2$ separated by distance r

$$W_D = \frac{\mathbf{d}_1\mathbf{d}_2 - 3(\mathbf{d}_1\mathbf{n})(\mathbf{d}_2\mathbf{n})}{r^3} \sim \frac{1}{r^3} \qquad (4)$$

depends sufficiently upon the molecules relative position. Here $\mathbf{n}$ is the unit vector directed along the line between molecules.

In order to reach the potential minimum, dipoles tend to align along the common axis **(Fig. 1)**. The thermal motion, however, breaks this order. To determine the "resulting" orientation potential W_{orient} one should average statistically interactions over all possible orientations of molecules pair. Notice that in accordance with the Gibbs distribution $\exp(-W/kT)$, which gives the probability of the system being in the state with energy W at temperature T, the energetically advantageous orientations are preferable. That is why despite the isotropy of possible mutual orientations, the average result will be nonzero.

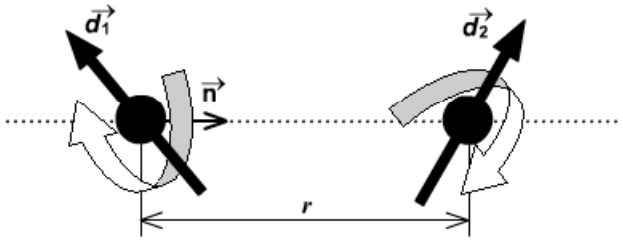

Averaging with the use of the Gibbs distribution is performed in accordance with the following formula:

$$W_{\text{orient}} = \frac{\int W_D \exp\left(-\frac{W_D}{kT}\right) dv}{\int \exp\left(-\frac{W_D}{kT}\right) dv} \qquad (5)$$

where, for the sake of normalization, the denominator is the statistical sum and v is the integration parameter providing enumeration of all the system possible states (a pair of dipoles mutual orientations).

If $W_D \ll kT$ the exponent can be approximated by the series expansion:

$$\exp\left(-\frac{W_D}{kT}\right) \approx 1 - \frac{W_D}{kT} \qquad (6)$$

so the energy of orientation interaction is approximated as:

$$W_{\text{orient}} \sim \frac{\int W_D dv + \int \frac{W_D^2}{kT} dv}{\int dv + \int W_D dv} \qquad (7)$$

On performing integration it can be shown that $\int W_D dv = 0$, thus, $W_{\text{orient}} \sim W_D^2$. Introducing constant A_1 in accordance with (4), we finally have:

$$W_{\text{orient}} = \frac{const}{kT}\frac{1}{r^6} = -\frac{A_1}{r^6} \qquad (8)$$

A few words on van der Waals II

The induction interaction (or the **Debye force**) arises between polar and nonpolar molecules. Electric field $\mathbf{E}$ generated by dipole $\mathbf{d}_1$ polarizes the other molecule **(Fig. 2)**. The induced moment calculated in the first order of the quantum perturbation theory is equal to $\mathbf{d}_{\text{ind}} = \chi\mathbf{E}$ where χ stands for the molecule polarizability.

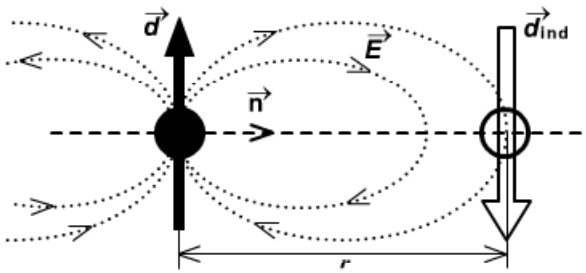

Then, the potential of induction interaction is computed as follows:

$$W_{\text{ind}} = \mathbf{d}_{\text{ind}}\mathbf{E} = \chi\mathbf{E}^2 = \chi\frac{-3(\mathbf{n}\mathbf{d}_1)^2 + \mathbf{d}_1^2}{r^6} = -\frac{\chi\mathbf{d}_1^2}{2r^6} \sim \frac{1}{r^6} \qquad (9)$$

Thus, this kind of interaction also "universally" depends on $W = W_{\text{orient}} + W_{\text{ind}} + W_{\text{disp}} \sim 1/r^6$ though having the other reason and the other constant.

It should be noted that in liquids and solids the polarized molecule experiences the symmetric influence of many neighbor molecules, the induction interaction being strongly compensated by their action. The result is that the real induction interaction is estimated as:

$$W_{\text{ind}} \sim \frac{1}{r^n},\ n = 8 \div 13 \qquad (10)$$

Obviously, the force is determined by

$$\mathbf{F} = -\operatorname{grad} W_D\ ,\ W_{\text{disp}} = -\frac{A_3}{r^6} \qquad (13)$$

Estimations of the Van der Waals attraction for AFM studies in the contact mode give: $F_{\text{VdV}} \sim 10^{-8} \div 10^{-9}$ N.

Van der Waals interaction is based on different dipole/dipole interaction mechanisms, all leading to a r^{-6} behavior

This results into a r^{-m} force on the cantilever depending on specific tip shape and distance

The dispersion interaction (or the **London force**) is a prevailing one because it involves nonpolar molecules as well. This third term in (1) is always presented that is why it is the major one.

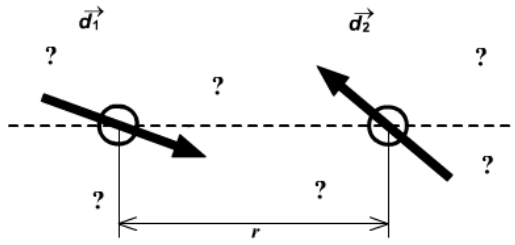

Fig. 3. Due to the quantum uncertainty, nonpolar molecules have "momentary" dipole moments, interaction between which is of the second order of smallness of the perturbation theory.

In a system of nonpolar molecules the electrons wave function Ψ is such that average values of dipole moments in any state n are equal to zero: $\langle\psi_n|\mathbf{d}_{1,2}|\psi_n\rangle = 0$. However, nondiagonal matrix elements $\langle\psi_n|\mathbf{d}_{1,2}|\psi_m\rangle$ are nonzero. Moreover, the second quantum mechanical correction to the interaction energy calculated as is known [2] according to the formula below, is nonzero too:

In a system of nonpolar molecules the electrons wave function Ψ is such that average values of dipole moments in any state n are equal to zero: $\langle\psi_n|\mathbf{d}_{1,2}|\psi_n\rangle = 0$. However, nondiagonal matrix elements $\langle\psi_n|\mathbf{d}_{1,2}|\psi_m\rangle$ are nonzero. Moreover, the second quantum mechanical correction to the interaction energy calculated as is known [2] according to the formula below, is nonzero too:

$$W_n^{(2)} = \sum_{n,m}\frac{|\langle\psi_n|W|\psi_m\rangle|^2}{\varepsilon_n - \varepsilon_m} \qquad (11)$$

where perturbation W is given by (4), ε_n, ε_m – energies of the system of two molecules in arbitrary states n and m.

In a certain sense, "momentary" magnitudes of dipole moments (at zero average value) are nonzero and they interact **(Fig. 3)**. In the second order of smallness the averaged magnitude of such "momentary" potential is not already vanished and namely this is the potential of dispersion interaction.

Correction (11) as is seen, is proportional to the square of perturbation W_D. From this it is clear that

$$W_{\text{disp}} \sim W_D^2\ ,\ W_{\text{disp}} = -\frac{A_3}{r^6} \qquad (12)$$

Constant $A_3 = \frac{3I_1I_2}{2(I_1+I_2)}\chi_1\chi_2$ is called the Hamaker constant (here I_1, I_2 – ionization potentials, χ_1, χ_2 – molecules polarizability).

The classical interpretation of this interaction is as follows. The dipole moment of one molecule arisen from fluctuations, generates field which, in turn, polarizes the second molecule. The already nonzero field of the second molecule polarizes the first one. The potential of this peculiar system with a "positive feedback" is calculated similarly to the induction interaction.

Hertz problem (continuous)

When the cantilever and the sample are in contact, elastic forces start to act giving rise to both the sample and tip deformations which can affect the acquired image. To properly interpret the results and choose the measuring mode one should have a clear idea of elastic interactions in contact and "semicontact" modes.

Such consideration is necessary in order to:

- avoid tip or sample damage during scanning - even at low loading force the pressure in a contact zone can exceed the strength limit because contact area is very small.
- reconstruct properly the sample surface topography basing on the acquired image profile in case when surface features are of the same size as the tip curvature radius.
- analyze forces in the "semicontact" mode at a moment of the tip contact with the surface which directly affect the cantilever oscillation and are one of the damping reasons.

Elastic deformations in the contact zone (the Hertz problem).

Hertz problem

Let us consider first only the elastic force. **The Hertz problem** is deformations determination at local contact of bodies under load F action.

We have to adopt some simplifying assumptions [1].

1. Suppose that both the cantilever and sample materials are isotropic, i.e. their elastic properties are described only by two pairs of parameters – Young's moduli E, E' and Poisson ratios μ, μ'. (For the anisotropic materials the number of such independent elastic characteristics can reach 21).
2. Assume that in the vicinity of the contact point the undeformed parts of bodies surface in perpendicular planes orthogonal to the plane in the given point **(Fig. 1)** are described by two curvature radii r_1, r_2 (for the tip) and r_1', r_2' (for the studied sample area).
3. Deformations are small compared to surfaces curvature radii.

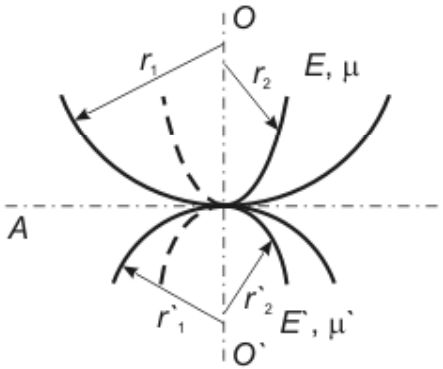

Fig. 1. Hertz problem definition.

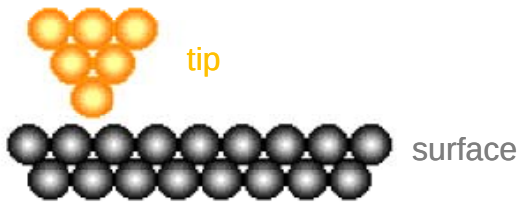

Solution in spherical simmetries

The general solution to this problem is well known (see chapter 2.2.2.3) though it is written in an implicit form [1]. In order to get the general idea of the deformations in elastic contact and obtain characteristic numerical values, we will confine to the analysis of two spherical surfaces interaction – the tip and the small sample area. This means that $r_1 = r_2 = r$, $r_1' = r_2' = r'$.

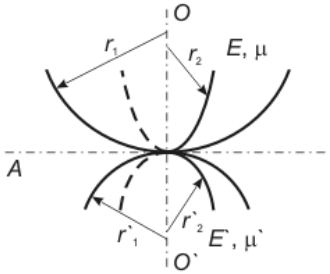

Fig. 1. Hertz problem definition.

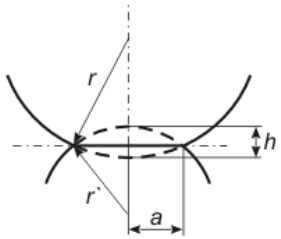

Fig. 2. Relation between contact area radius a and penetration depth h in deformed state.

Under the load the contacting bodies deform in such a way that instead of a contact point some contact area arises. Since the problem symmetry is axial, this area is clearly circular. Denote its radius by a.

Let us introduce the following convenient quantities: $1/R = 1/r + 1/r'$ and effective Young's modulus of the given pair of materials:

Effective Young's modulus for the material pair (springs in series)

$$\frac{1}{K} = \frac{3}{4}\left(\frac{1-\mu'^2}{E'} + \frac{1-\mu^2}{E}\right) \qquad (1)$$

At small deformations (assumption 3 in chapter 2.2.2.1) the following geometric relation between penetration depth h and contact circle radius a is valid:

$$h = \frac{a^2}{R} \qquad (2)$$

which is clear from Fig. 2.

The Hertz problem solution relates the loading force F and the penetration depth h:

$$\boxed{F = \frac{Ka^3}{R} = Kh^{\frac{3}{2}}R^{\frac{1}{2}}} \qquad (3)$$

Accordingly, the pressure is the following function of the force:

$$P = \frac{F}{\pi a^2} = \frac{1}{\pi}\sqrt[3]{\frac{FK^2}{R^2}} \qquad (4)$$

Hertz II

The given solution for the case of two spherical bodies contact includes one important special case of the flat sample contact with the tip having curvature radius R ($r = R$, $r' = \infty$).

Let us depict the Hertz problem solution, i.e. the dependence of the penetration depth (horizontal axis) upon the loading force (vertical axis) for positive h. In **Fig. 3**, the rising branch corresponds to the Hertz problem solution.

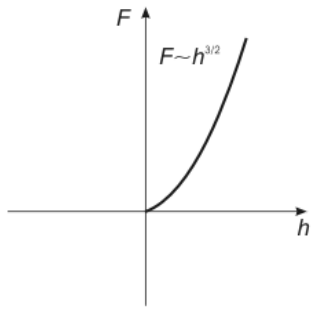

Fig. 3. Force F depending on penetration depth h (graph of the Hertz problem solution).

As mentioned above, the solution can be obtained in implicit form for any kind of surfaces (stipulated in condition 2 in chapter 2.2.2.1), however our goal is an exact numerical result. Nevertheless, this result by the order of magnitude is the same as in our simplified case. Therefore, we can estimate the characteristic contact pressure from formula (4).

Results are tabulated in tables which present magnitudes of contact area and pressure at various Young's modulus of a studied material. The data are calculated for the silicon cantilever – $E = 150\,\mathrm{GPa}$ – with the curvature radius $10\,\mathrm{nm}$ at two loading force magnitudes $F = 5\cdot 10^{-9}\,\mathrm{N}$ and $F = 5\cdot 10^{-8}\,\mathrm{N}$.

Sample Young's modulus, Pa	Contact area radius a, nm		Penetration due to deformation h, nm		Contact pressure p, GPa	
10^8	7.2	16	5.2	24	0.03	0.07
10^9	3.4	7.2	1.1	5.2	0.14	0.3
10^{10}	1.6	3.4	0.25	1.1	0.63	1.4
10^{11}	0.9	1.8	0.07	0.3	2.2	4.7
10^{12}	0.7	1.4	0.04	0.2	3.7	7.9
at loading force F, nN						
	5	50	5	50	5	50

Table 1. Comparative analysis of contact deformations arising during AFM-investigation of materials having different elastic properties [2].

Material and its Young's modulus	Contact area radius a, nm		Penetration due to deformation h, nm		Contact pressure p, GPa	
Quartz glass, $E = 0.65\,\mathrm{GPa}$	3.74	8.04	1.04	6.46	0.11	0.25
Kapron, $E = 1\,\mathrm{GPa}$	3.24	6.98	1.05	4.87	0.15	0.33
Copper, $E = 120\,\mathrm{GPa}$	0.79	1.7	0.062	0.29	2.55	5.51
Tungsten, $E = 400\,\mathrm{GPa}$	0.68	1.46	0.046	0.21	3.44	7.47
Diamond, $E = 1000\,\mathrm{GPa}$	0.64	1.38	0.041	0.19	3.88	8.36
at loading force F, nN						
	5	50	5	50	5	50

Table 2. Comparative analysis of contact deformations arising during AFM-investigation of materials having different elastic properties using silicon cantilever.

It is clearly seen that the contact pressure is higher for more stiff samples.

The other restriction (assumption 1 in section 2.2.2.1) is the problem solution within the model of the continuum with isotropic characteristics. Naturally, on the microlevel, the molecular structure is of great importance, therefore such assumption is rather relative. That is why the Hertz problem solution with a more exact geometrical characteristics of contacting surfaces (in contrast to the considered case) makes no sense because assumption 1 in section 2.2.2.1 itself is a very crude approximation.

Summary.

- The Hertz problem allows to determine parameters of deformation in a "point" of two bodies contact.
- Definition of the Hertz problem implies the use of uniform isotropic linearly elastic media model and the assumption of deformations smallness.
- In a place of the tip-sample "point" contact the contact area arises.
- The Hertz problem solution relates the deformation and applied load. Penetration h is proportional to the compressing force as $F^{2/3}$.

Forces in AFM

Materials destruction during scanning.

Once the contact pressure is estimated according to formula (4) in chapter 2.2.2.2, it is easy to determine which material can be damaged during scanning. For that it is enough to compare materials ultimate strength (measured in Pa) and arising stress (pressure P). See Appendix 1.

However, even if this strength is exceeded, no probe or sample material destruction can occur during scanning. The point is that the overcritical pressure should act longer than the damage process duration (relaxation time of elastic deformations is about 10^{-6} s). During rather fast scanning of large areas this condition may fail. See Appendix 2.

Reconstruction of the surface feature shape from the scan line profile.

The change in the probe vertical position during scanning in the contact mode produces profile which can differ much from the real surface topography. One of the reasons for that is the elastic deformation of the tip and the sample. For example, the decrease in the organic molecules vertical dimensions was experimentally established. Because these materials are very soft, the probe "indents" protrusions on their surfaces (See Appendix 3 and chapter 2.5.1).

The second reason for the difference between scan profile and real surface geometry is the tip-sample convolution. Its consideration is important when studying small (of the order of the tip curvature radius) surface features. A finite tip dimension results in the lack of the ability to probe narrow cavities on the sample surface thus decreasing their depth and width. Similarly, convex features image appears wider. The convolution phenomenon is best understood from **Fig. 1**.

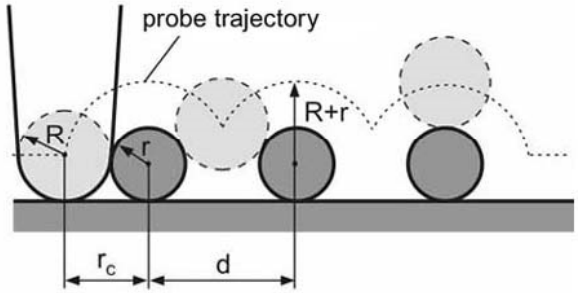

Fig. 1. Tip convolution during scanning. The scan profile can differ much from real surface geometry.

It can be seen that for an object having in reality radius $r \sim R$ the measured dimensions are larger depending on the tip radius (see details in the chapter 2.5.2).

If one assumes the simultaneous effect of convolution and deformation, it becomes clear how much the image profile can differ from the real topography. In Appendix 4 it is demonstrated that the acquired image needs to be analyzed and even computer processed in order to obtain the sample real topography.

Non-elastic conservative contact forces.

As tip makes contact with the sample, some other forces arise besides the elastic one. For example, the Van der Waals interaction (revealed not only when two bodies touch but within some distance between them) leads to the contact pressure decrease because Van der Waals forces in contrast to elastic ones are attractive but not repulsive.

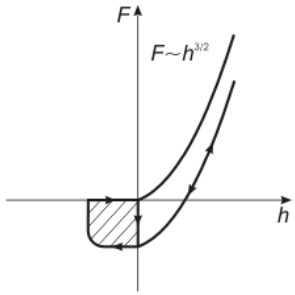

Fig. 2. Plots of force F vs. penetration depth h. Shown are the Hertz problem solution as well as solution with a hysteresis loop accounting for the nonconservative forces.

This alongwith other attractive microscopic interactions (not discussed here) result in the downward shift of the plot (Fig. 3 in chapter 2.2.2.2) which illustrates the Hertz problem solution. As can be seen, at $h = 0$ the force is negative. This means that as the tip slightly touches the sample, an attractive force acts.

Nonconservative effects.

Besides elastic and Van der Waals forces, some other nonconservative forces exist: from friction to energy dissipation by arising elastic waves a phononos. These forces modify the Hertz problem solution even greater. Let us consider the experimental consequences of such contact interactions.

Particularly, due to the nonconservative forces, the tip adhesion (sticking to the surface) takes place. In this case the touch and separation happen differently, i.e. the hysteresis occurs.

The tip adhered to the surface carries a small "stuck" portion of the sample (during the upward move) which, for some time before separation, goes up producing a neck **(Fig. 3)**.

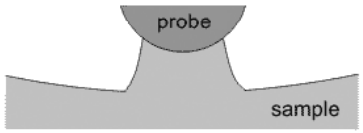

Fig. 3. "Sticking" of the sample surface portion to the tip is due to nonconservative forces and results in hysteresis.

The hysteresis loop in the plot means that in order to press the tip into the sample surface and then separate it and bring it back, some work must be done. In other words, if one hits the sample surface with the cantilever, the collision will be non-elastic. In semicontact vibration mode such non-elastic sticking is one of the damping factors.

Not to forget: adhesion/capillary effects

Let us examine the effect of the surface tension on AFM measurements. [1]At the moment of a cantilever contact with a liquid film on a flat surface, the film surface reshapes producing the **"neck"**. The water wets the cantilever surface **(Fig. 1)** because the water-cantilever contact (if it is hydrophilic) is energetically advantageous as compared to the water-air contact. Notice that in such cases the contact angle is always less than $90°$.

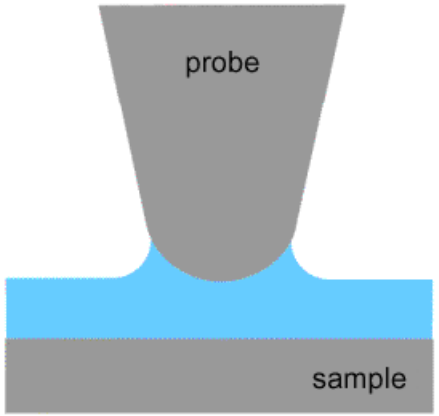

Fig. 1. "Neck" formation.

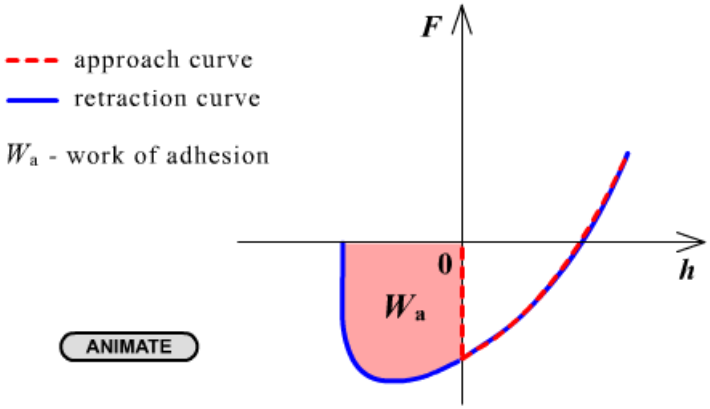

It is intuitively clear that the neck curved surface will tend to flatten that is available only at the expense of the cantilever pulling down. This means that the cantilever attracts to the sample.

Calculation of this attraction force is a simple task. Let the tip curvature radius be much larger than other characteristic dimensions of the case. In **Fig. 2** the following designations are introduced: D – tip-sample separation, d – "immersion depth", h – film thickness, ρ_1 – lesser curvature radius of the liquid surface, ρ_2 – tip-liquid contact area radius.

We will not concentrate attention on d value determination. For the estimation purpose we will use the maximum value of the capillary attraction force that takes place at $D = 0$. In this case the unknown parameter d vanishes:

$$F_{cap} = F_{max} = 4\pi R\sigma\cos\theta \qquad (5)$$

Taking into account that cantilever radius R is $10\,\text{nm}$, water surface tension at $20°C$ is equal to $0.073\,\text{N/m}$ and the contact angle is small i.e. $\cos\theta$ is close to 1, we get the following estimation: $F_{cap} \sim 10^{-8} - 10^{-9}\,\text{N}$. Thus, the capillary force by the order of magnitude is the same as the Van der Waals interaction and the electrostatic force.

During the cantilever approach-retraction cycle, the hysteresis arises. At the upward move the neck stays longer because the cantilever surface is already wetted and the liquid neck goes with the tip. As bonds break, the capillary force stops to act and the cantilever suddenly returns into its undeflected state.

Adhesion effects can further affect the interaction (unless UHV operation is performed!)

Scanning Force Microscopy

3.2 The Operation Principle of Scanning Force Microscope

The main electronic components of the SFM are the same as for the STM, only the topography of the scanned surface is reconstructed by analysing the deflection of the tip at the end of a spring. Today, the interferometrical and optical lever method dominate commercial SFM apparatus. The most common method for detecting the deflection of cantilever is by measuring the position of a reflected laser-beam on a photosensitive detector. The principle of this optical lever method is presented in Figure 18 a. Without cantilever displacement both quadrants of the photodiode (A and B) have the same irradiation $P_A = P_B = P/2$ (P represents the total light intensity). The change of the irradiated area in the quadrants A and B is a linear function of the displacement

$$\delta \propto \Delta d = 2\sin(\Theta)\cdot S_2 \approx 2\Theta \cdot S_2 = 3S_2 \cdot \delta / L \qquad (10)$$

For small angles $\sin(\Theta) \approx \Theta$ and Θ may be evaluated from the relation $\Theta = 3\delta/2L$ (Figure 18b). For P_A and P_B one would get approximately $P_A = P/2\cdot(d+\Delta d)/2$ and $P_B = P/2\cdot(d-\Delta d)/2$. Using the simple difference between P_A and P_B would lead to $\Delta P = P\cdot 3S\delta/(Ld)$ but in this case one cannot distinguish between the displacement δ of the cantilever and the variation in the laser power P. Hence the normalised difference is used, which is only dependent of δ:

$$\frac{P_A - P_B}{P_A + P_B} = \delta \cdot \frac{3S_2}{Ld} \qquad (11)$$

The "lever amplification" $\Delta d/\delta = 3S_2/L$ is about a factor of one thousand. On the basis of this kind of technique one is able to detect changes in the postion of a cantilever of the order of 0.01 nm.

For large distances between the tip and the sample the bending of the cantilever by attractive forces is negligible. After the cantilever is brought closer to the surface of the sample (point "a" Figure 18c) the van der Waals forces induce a strong deflection of the cantilever and, simultaneously, the cantilever is moving towards the surface. This increases the forces on the cantilever, which is a kind of positive feedback and brings the cantilever to a direct contact with the sample surface (point "b"). However, when the cantilever is brought even closer in contact to the sample, it actually begins to bend in the opposite direction as a result of a repulsive interaction ("b-c"). In the range ("b-c") the position of the laser beam on both quadrants, which is proportional to the force, is a linear function of distance. On reversal this characteristic shows a hysteresis. This means that the cantilever loses contact with the surface at a distance (point "d") which is much larger than the distance on approaching the surface (point "a").

Up to now, the actual probe, i.e. the tip of the leaf spring, has not been discussed in detail. Its preparation is particularly demanding since the tip and the sensitive spring should be one piece. Moreover, the cantilever should be as small as possible. Nowadays, such scanning tips are commercially available (in contrast to the tunnelling tips, which you should prepare yourself). Figure 19 shows such a spring with tip (cantilever) made of Si. The characteristic parameters of a cantilever has been presented in Figure 18b. The spring constant $k = Ead_c^3/4L^3 \sim 0.1 - 10$ N/m of the cantilever enables topographical analysis with atomic resolution.

For the realisation of a scanning force microscope, the force measurement must be supplemented by a feedback control, in analogy to the scanning tunnelling microscope. The controller keeps the amplitude of the vibration of the cantilever (the tip), and thus also the distance, constant. During scanning the feedback controller retracts the sample with the scanner of a piezoelectric ceramic or shifts towards the cantilever until the vibration amplitude has reached the setpoint value again. The principle of height regulation is exactly the same as for the scanning tunnelling microscope. *The scanning force micrographs thus show areas of constant effective force constant.* If the surface is chemically homogeneous and if only van der Waals forces act on the tip, the SFM image shows the *topography of the surface.*

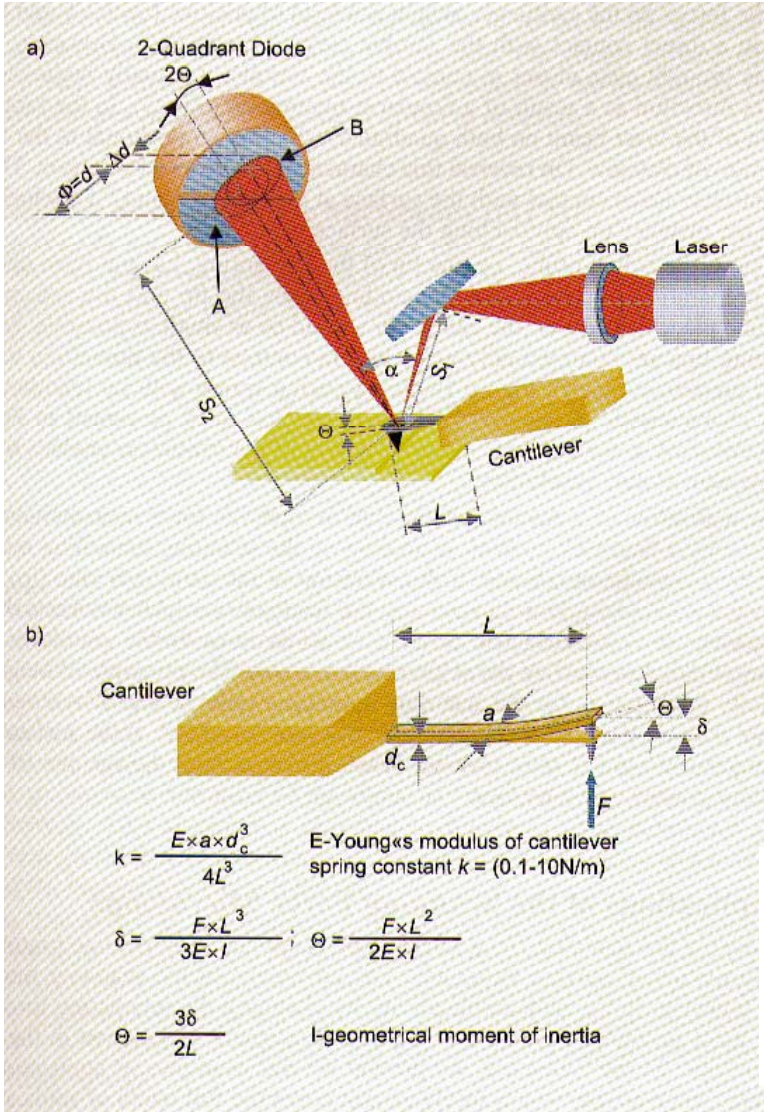

Figure 18: The amplification of the cantilever motion through the optical lever arm method.
(a) Optical laser path in the standard AFM set-up.
(b) Cantilever beam in bending.
(c) Cantilever force as a function of the distance tip – sample distance.

An optical lever method is used to detect the cantilever deflection

Force vs distance curves

In the approaching step, force (i.e., cantilever deflection) vs distance plots have a typical behavior

Force vs distance curves can be used to get local information on the mechanical properties of the surface (*force spectroscopy*)

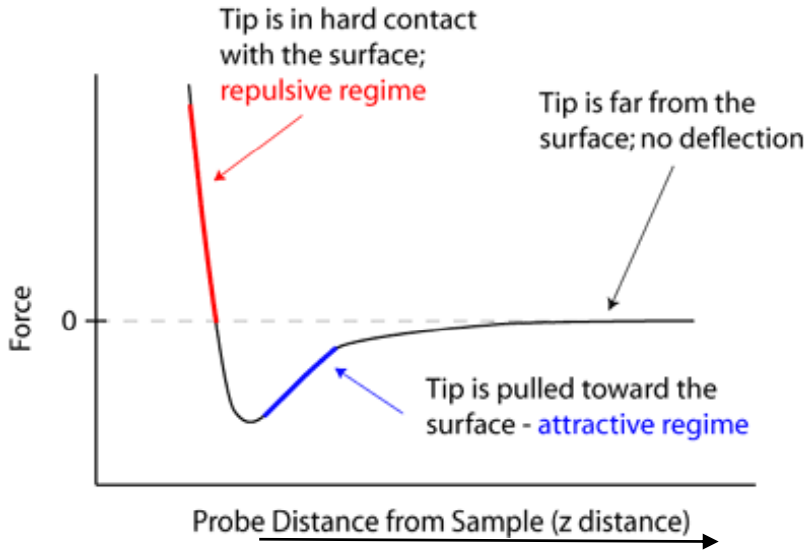

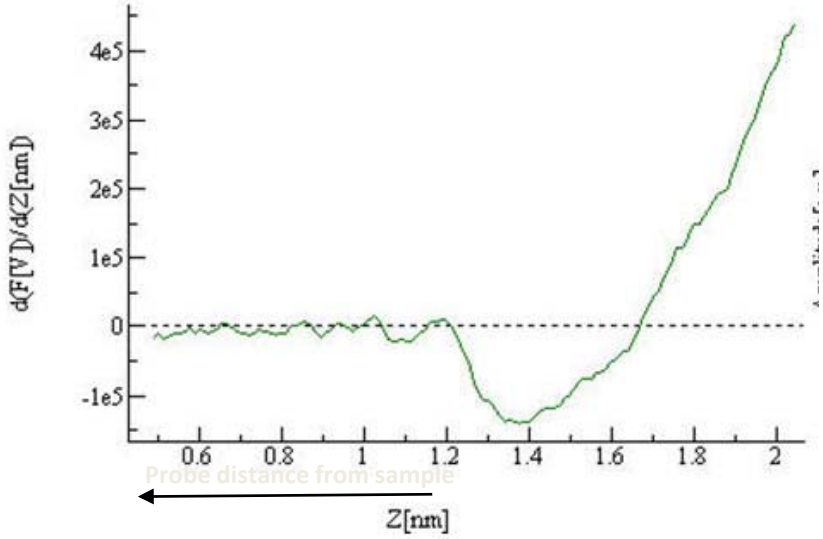

Note: we are discussing of the **contact mode operation** and tip might penetrate into the sample (*as in nanoindentation – we will see later!)*

Contact mode of operation

3.1 Theoretical Principles of the Scanning Force Microscope

As already mentioned above, van der Waals forces lead to an attractive interaction between the tip on the spring and the sample surface. Figure 15 shows schematically the van der Waals potential between two atoms. The potential can be described in a simpler classical picture as the interaction potential between the time dependent dipole moments of the two atoms. Although the centres of gravity of the electronic charge density and the charge of nucleus are exactly overlapping on a time average, the separation of the centres of gravity is spatially fluctuating in every moment. This produces statistical fluctuations of the atoms' dipole moments. The dipole moment of an atom can again induce a dipole moment in the neighbouring atom and the induced dipole moment acts back on the first atom. This creates a dipole-dipole interaction on basis of the fluctuating dipole moments. This interaction decreases with d^{-6} in the case of small distances d (Lenard-Jones potential). At larger distances, the interaction potential decreases more rapidly (d^{-7}). This arises from the fact that the interaction between dipole moments occurs through the exchange of virtual photons. If the transit time of the virtual photon between atoms 1 and 2 is longer than the typical fluctuation time of the instantaneous dipole moment, the virtual photon weakens the interaction. This range of the van der Waals interaction is therefore called retarded, whereas that at short distances is unretarded.

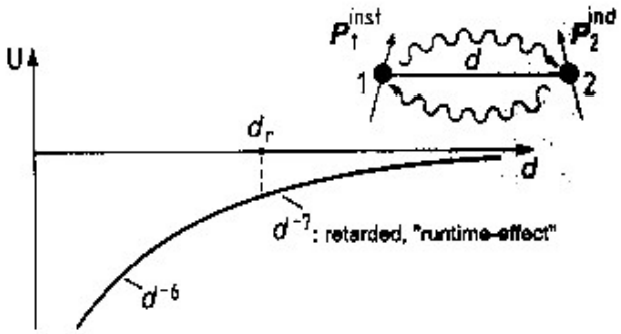

Figure 15: The van der Waals potential U between two atoms. d_r is the critical distance above which the transit time effects weaken the interaction [23].

The scanning force microscope is not based on the interaction of individual atom only. Both the sample and the tip are large in comparison to the distance. In order t obtain their interaction, all forces between the atoms of both bodies need to be inte grated. The result of this is known for simple bodies and geometries. In all cases, th summation leads to a weaker decrease of the interaction. A single atom at distance d re ative to a half-space leads to an interaction potential of

$$U = -\frac{C\pi\rho}{6}\cdot\frac{1}{d^3} \quad (7$$

where C is the interaction constant of the van der Waals potential and Δ the density o the solid. C is basically determined by the electronic polarizabilities of the atoms in th half-space and of the single atom. If one has two spheres with radii R_1 and R_2 at distanc d (distance between sphere surfaces) one obtains an interaction potential of

$$U = -\frac{AR_1R_2}{6(R_1+R_2)}\cdot\frac{1}{d} \quad (8$$

where A is the so-called Hamaker constant. It is materials specific and essentially con tains the densities of the two bodies and the interaction constant C of the van der Waal potential. If a sphere with radius R has a distance d from a half-space, an interactior potential of

$$U = -\frac{AR}{6}\cdot\frac{1}{d} \quad (9)$$

Realistic tip/surface potential

is obtained from Eq. (8). This case describes the geometry in a scanning force microscope best and is most widely used. The distance dependence of the van der Waals potential thus obtained is used analogously to the distance dependence of the tunnel current in a scanning tunnelling microscope to achieve a high resolution of the scanning force microscope. However, since the distance dependence is much weaker, the sensitivity of the scanning force microscope is lower.

Contact mode is suitable for rather rigid surfaces

In the contact mode of operation, mechanical interaction leads to tip displacement, i.e., to cantilever deflection related to topography changes

As in STM (constant gap), typical operation foresees a **feedback** system, acting on the *Z* direction of the piezoscanner, which keeps constant the cantilever deflection during the scan

The "error signal" of the feedback system provides a **topography map (with a calibrated sub-nm space resolution)**

Operation modes (AFM contact)

The most straightforward AFM operation mode involves "**contact**" (repulsive) forces
Constant height and **constant force** configurations are possible (the latter, the most common, is based on feedback)
Major drawback: surface degradation, especially with soft matter

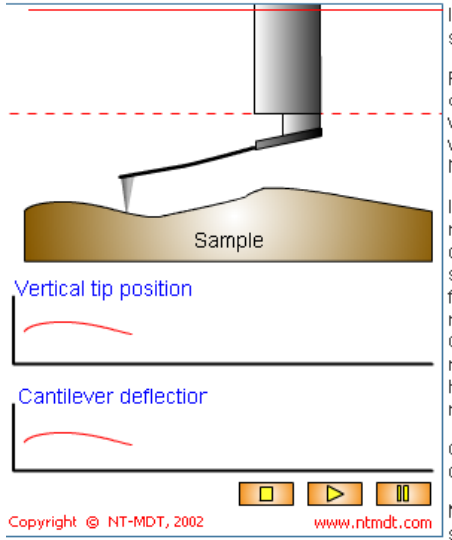

In Contact mode of operation the cantilever deflection under scanning reflects repulsive force acting upon the tip.

Repulsion force F acting upon the tip is related to the cantilever deflection value x under Hooke's law: F = -kx, where k is cantilever spring constant. The spring constant value for different cantilevers usually vary from 0.01 to several N/m.

In our units the vertical cantilever deflection value is measured by means of the optical registration system and converted into electrical signal DFL. In contact mode the DFL signal is used as a parameter characterizing the interaction force between the tip and the surface. There is a linear relationship between the DFL value and the force. In Constant Height mode of operation the scanner of the microscope maintains fixed end of cantilever on the constant height value. So deflection of the cantilever under scanning reflects topography of sample under investigation.

Constant Height mode has some advantages and disadvantages.

Main advantage of Constant Height mode is high scanning speeds. It is restricted only by resonant frequency of the cantilever.

Constant Height mode has also some disadvantages. Samples must be sufficiently smooth. When exploring soft samples (like polymers, biological samples, Langmuir-Blodgett films etc.) they can be destroyed by the scratching because the probe scanning tip is in direct contact with the surface. Thereunto under scanning soft samples with relatively high relief the pressure upon the surface varies , simultaneously varies local flexure of sample surface. As a result acquired topography of the sample can prove distorted. Possible existence of substantial capillary forces imposed by a liquid adsorption layer can decrease the resolution.

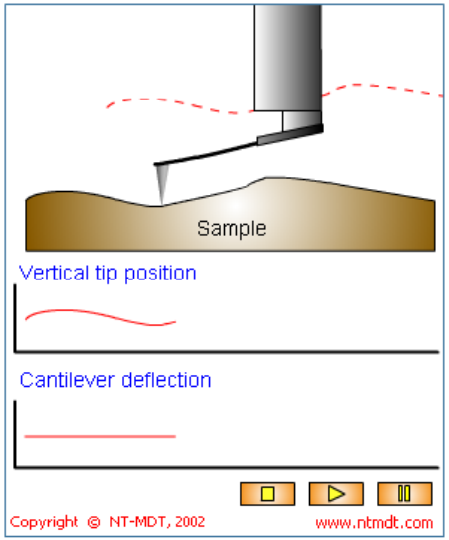

In Contact mode of operation the cantilever deflection under scanning reflects repulsive force acting upon the tip.

Repulsion force F acting upon the tip is related to the cantilever deflection value x under Hooke's law: F = -kx, where k is cantilever spring constant. The spring constant value for different cantilevers usually vary from 0.01 to several N/m.

In our units the vertical cantilever deflection value is measured by means of the optical registration system and converted into electrical signal DFL. In contact mode the DFL signal is used as a parameter characterizing the interaction force between the tip and the surface. There is a linear relationship between the DFL value and the force. In Constant Force mode of operation the deflection of the cantilever is maintained by the feedback circuitry on the preset value. So vertical displacement of the scanner under scanning reflects topography of sample under investigation.

Constant Force mode has some advantages and disadvantages.

Main advantage of Constant Force mode is possibility to measure with high resolution simultaneously with topography some other characteristics - Friction Forces, Spreading Resistance etc.

Constant Force mode has also some disadvantages. Speed of scanning is restricted by the response time of feedback system. When exploring soft samples (like polymers, biological samples, Langmuir-Blodgett films etc.) they can be destroyed by the scratching because the probe scanning tip is in direct contact with the surface. Thereunto under scanning soft unhomogeneous samples the local flexure of sample surface varies. As a result acquired topography of the sample can prove distorted. Possible existence of substantial capillary forces imposed by a liquid adsorption layer can decrease the resolution.

Locally probing the (repulsive) force allows for topography and morphology reconstruction

Non-contact modes of operation

The dynamic operation method of a scanning force microscope has proved to be particularly useful. In this method the nominal force constant of the van der Waals potential, i.e. the second derivative of the potential, is exploited. This can be measured by using a vibrating tip (Figure 16). If a tip vibrates at distance d, which is outside the interaction range of the van der Waals potential, then the vibration frequency and the amplitude are only determined by the spring constant k of the spring. This corresponds to a harmonic potential. When the tip comes into the interaction range of the van der Waals potential, the harmonic potential and the interaction potential are superimposed thus changing the vibration frequency and the amplitude of the spring.

This is described by modifying the spring constant k of the spring by an additional contribution f of the van der Waals potential. As a consequence, the vibration frequency is shifted to lower frequencies as shown in Figure 17. ω_0 is the resonance frequency without interaction and $\Delta\omega$ the frequency shift to lower values. If an excitation frequency of the tip of $\omega_m > \omega_0$ is selected and kept constant, the amplitude of the vibration decreases as the tip approaches the sample, since the interaction becomes increasingly stronger. Thus, the vibration amplitude also becomes a measure for the distance of the tip from the sample surface. If a spring with low damping Q^{-1} is selected, the resonance curve is steep and the ratio of the amplitude change for a given frequency shift becomes large.

In practice, small amplitudes (approx. 1 nm) in comparison to distance d are used to ensure the linearity of the amplitude signal. With a given measurement accuracy of 1 %, however, this means that the assembly must measure deflection changes of 0.01 nm, which is achieved most simply by a laser interferometer or optical lever method.

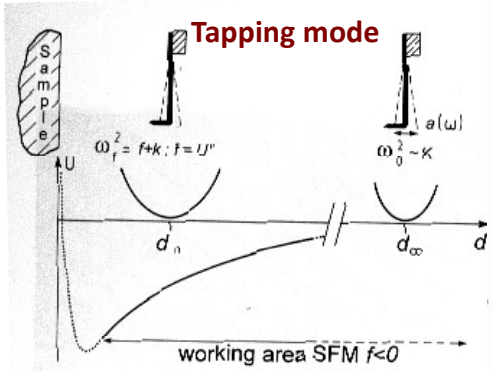

Figure 16: Schematic representation of the effect of the van der Waals interaction potential on the vibration frequency of the spring with tip. As the tip approaches the surface, the resonance frequency of the leaf spring is shifted. (from [23]).

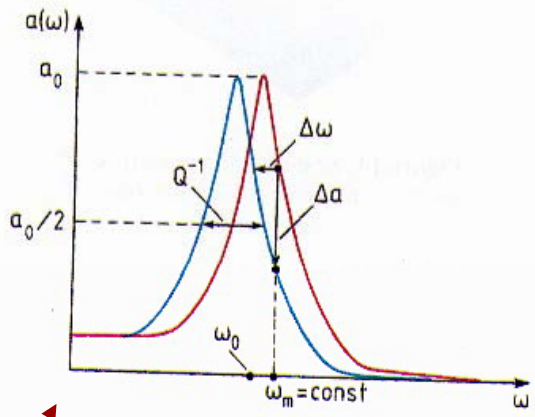

Figure 17: Resonance curves of the tip without and with interaction with a van der Waals potential. The interaction leads to a shift $\Delta\omega$ of the resonance frequency with the consequence that the tip excited with the frequency ω_m has a vibration amplitude $a(\omega)$ attenuated by Δa [23].

In **non-contact (tapping) mode**, the tip/sample distance is continuously modulated thanks to a vibrating tip

Tip vibration is typically achieved by using a piezoelectric transducer fed by an oscillating voltage and mechanically coupled to the cantilver

Oscillation frequency is typically set around the mechanical resonance frequency of the system (cantilever+tip), i.e., hundreds of kHz

The vibration reflects in an oscillation of the position-sensitive detector (multiquadrant diode) and amplitude is monitored

Tip/sample interaction leads to a **damping** (and **phase shift**) of the recorded oscillation when the distance gets small

Suitably conditioned electronic signals are sent into the feedback system in order to stabilize the distance and to derive the topography map

Non-contact modes suitable for "soft" surfaces

No sample preparation is needed!!

Effects on the cantilever resonance

Consider a cantilever oscillations when in addition to driving force ((1) in chapter 2.2.3.3), an external force $F_{ts}(z)$ acts on it. The equation of motion in this case is written as

$$\ddot{z} + 2\delta\dot{z} + \omega_0^2 z = A_0 \cos \Omega t + F_{ts}(z)/m \qquad (1)$$

In a general case the steady-state solution of equation (1) is the sum of harmonics with frequencies divisible by a driving force frequency Ω:

$$z(t) = \sum_n A_n \cos\left(n\Omega t + \varphi_n\right) \qquad (2)$$

In chapter 2.2.3.4 we considered the particular case of equation (1) solution - **small oscillations** when the following condition is met

$$A_0 \ll \frac{m\omega_0^2}{\left\langle \frac{d^2 F_{ts}}{dz^2} \right\rangle} \qquad (3)$$

where ω_0 – cantilever natural resonant frequency, $\left\langle \frac{d^2 F_{ts}}{dz^2} \right\rangle$ – mean of the second derivative of the tip-sample interaction force (averaged with respect to oscillations amplitude.

In practice, condition (3) is seldom met. However, utilizing numerical methods, one can show that even under weak condition (4), the character of steady-state oscillations will only slightly differ from harmonic (a major contribution is made only by the first harmonic)

condition $$A_0 \le \frac{m\omega_0^2}{\left\langle \frac{d^2 F_{ts}}{dz^2} \right\rangle} \qquad (4)$$

solution $$z(t) \sim A\cos\left(\Omega t + \varphi\right) \qquad (5)$$

In contrast to the case of small oscillations where the steady-state condition is entirely determined by system parameters, the motion in the considered case depends on the initial state. That is, depending on the initial position of the cantilever relative to the equilibrium position, the character of the steady-state oscillations will vary (**Fig. 1**).

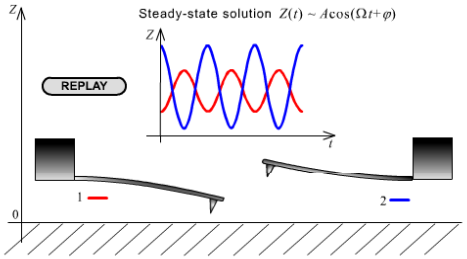

Fig. 1. Feasibility of several quasisteady-state solutions obtaining.

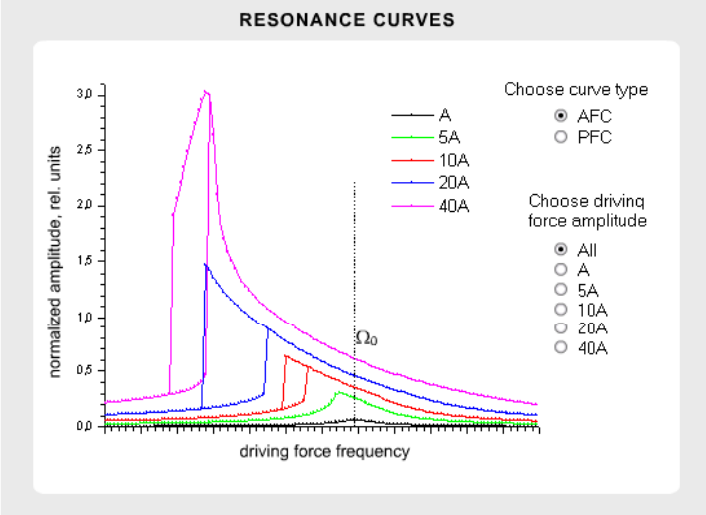

Fig. 2. Resonance curves in case of nonlinear oscillations.

Cantilever oscillatons are strongly dependent on "damping" (both in terms of amplitude and frequency/phase)

True non-contact mode

Non-Contact mode.

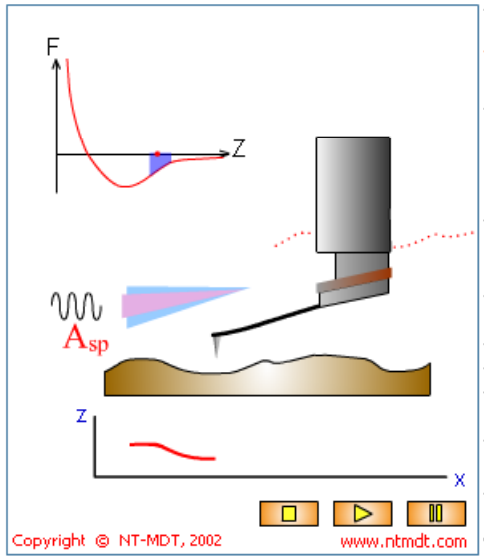

The Non-Contact AFM (NC AFM), invented in 1987 [1], offers unique advantages over other contemporary scanning probe techniques such as contact AFM and STM. The absence of repulsive forces (presenting in Contact AFM) in NC AFM permits it use in the imaging "soft" samples and, unlike the STM, the NC AFM does not require conducting samples.

The NC AFM works via the principle "amplitude modulation" detection. The corresponding detection scheme exploits the change in the amplitude, A, of the oscillation of a cantilever due to the interaction of a tip with a sample. To the first order, the working of the NC AFM can be understood in terms of a force-gradient model [1]. According to this model, in the limit of small A, a cantilever approaching a sample undergoes a shift, df, in its natural frequency, f_o, towards a new value given by

$$f_{eff} = f_o\,(1 - F'(z)/k_o)^{1/2}$$

where f_{eff} is the new, effective resonance frequency of the cantilever of nominal stiffness ko in the presence of a force gradient F'(z) due to the sample. The quantity z represents an effective tip-sample separation while $df = f_{eff} - f_o$ is typically negative, for the case of attractive forces.

If cantilever is initially forced to vibrate at a $f_{set} > f_o$, then the shift in the resonance spectrum of the cantilever towards lower frequencies will cause a decrease in the oscillation amplitude at f_{set} as the tip approaches the sample [1].

This change in A is used as the input to the NC-AFM feedback. To obtain a NC AFM image the user initially chooses a value A_{set} as the set-point such that $A_{set} < A(f_{set})$ when the cantilever is far away from the sample. The NC AFM feedback then moves the cantilever closer to the sample until its instantaneous oscillation amplitude, A, drops to A_{set} at the user-defined driving frequency f_{set}. At this point the sample can be scanned in the x–y plane with the feedback keeping $A = A_{set}$ = constant in order to obtain a NC AFM image. The NC AFM feedback brings the cantilever closer (on average) to the sample if A_{set} is decreased at any point, and moves the cantilever farther away from the sample (on average) if A_{set} is increased. Overall, the implication of the above model is that the NC AFM image may be considered, in the limit of small A, to be a map of constant interaction-force gradient experienced by the tip due to the sample.
The non-contact mode has the advantage that the tip never makes contact with the sample and therefore cannot disturb or destroy the sample. This is particularly important in biological applications.

References

1. J. Appl. Phys. 61, 4723 (1987).

- ✓ Vertical oscillation (tapping) is applied to the tip, at a frequency close to its resonance
- ✓ Resonance frequency variations (and dephasing) are measured
- ✓ Feedback keeps the resonance frequency constant by changing the probe/sample distance, hence topography is reconstructed

Non-contact modes allow for analysis of soft surfaces

Examples of other operation modes

Semicontact mode.

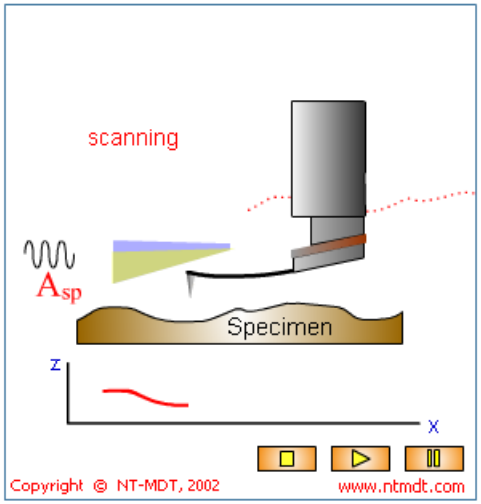

Usage of Scanning Force Microscopy with oscillating cantilever was firstly anticipated by Binnig [1]. Earlier experimental realizations of scanning with oscillated cantilever was realized in works [2, 3]. It was demonstrated influence of the force gradients on the cantilever frequency shift and possibility of non-contact scanning sample surface. It must be noted also that Durig studied frequency shift of oscillating cantilever under influence of STM tip [4].
In [2] was demonstrated also possibility of materials sensing under abrupt decreasing of cantilever oscillation amplitude. Possibility of scanning sample surface not only in attractive but also in repulsive forces was demonstrated in [4]. Relatively small shift of oscillating frequency with sensing repulsive forces means that contact of cantilever tip with sample surface under oscillation is not constant. Only during small part of oscillating period the tip "feels" contact repulsive force. Especially it concerns to oscillations with relatively high amplitudes. Scanning sample surface with cantilever oscillated in this manner is not non-contact, but intermittent contact. Corresponding mode of Scanning Force Microscope operation (Intermittent Contact mode) is in common practice.
The Intermittent Contact mode can be characterized by some advantages in comparison with dc Contact mode. First of all, in this mode the force of pressure of the cantilever onto the surface is less, that allows to work with softer and easy to damage materials such as polymers and bioorganics. The semicontact mode is also more sensitive to the interaction with the surface that gives a possibility to investigate some characteristics of the surface - distribution of magnetic and electric domains, elasticity and viscosity of the surface.

Semicontact: the tip gets in "temporarily" contact thus combining advantages of contact and non-contact

Force modulation: an additional contrast mechanism related to material (mechanical) properties is found and exploited

Force Modulation mode.

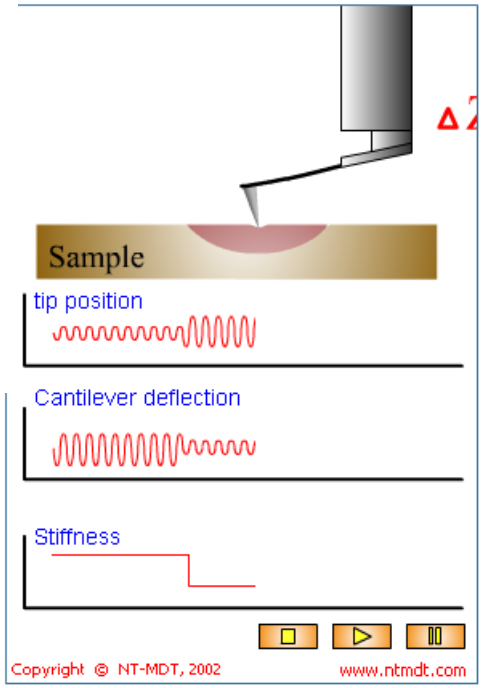

Under realization of Force Modulation mode (FM-mode) along with scanning of sample surface as in Constant Force mode (CFC-mode) the scanner (or the sample) executes a vertical periodic motion [1]. Under this periodic motion cantilever "feels out" the sample surface. At that the pressure of the probe tip on the sample surface does not remain constant but has periodic component, usually sinusoidal. In accordance with the local elasticity of the sample value of corresponding indentation will change under scanning. On the stiff areas of the sample surface depth of indentation will be smaller, and on the compliant areas - larger. Tracing of the sample surface relief height is conducted by the usage of the averaged cantilever deflection in the feedback circuit [2]. If values of the scanner vertical displacement Dz, the probe tip vertical displacement D and cantilever force constant κ_c are known, one can determine the local elasticity of the sample under investigation κ_s

$$\kappa_s = \kappa_c \cdot (Dz/D - 1)$$

In turn with known value of the local elasticity one can to determine the modulus of elasticity of the sample. It can be done with usage of the calibrating measurements or with usage of the Hertzian model [3]. Force Modulation mode is widely used in polymers, semiconductors, biological, especially in composite materials investigations.

A very few examples of AFM images I

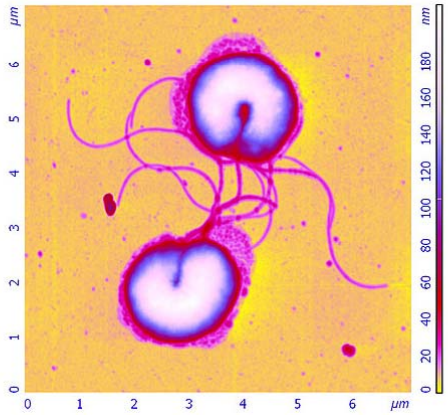

Helicobacter pylori

Mode: Semicontact mode
SPM Model: Solver P47H-PRO
Scan size: 7.2x7.2 µm
Source MDT-file: download (1.01 Mb)

Conversion of two cells of bacterium *Helicobacter pylori* into coccoid forms. Polished silicone covered by polymer.

Image courtesy of Budashov I.A., Moscow State University, Institute of Biochemical Physics.
Sample courtesy of Momynaliev K.T., Scientific Research Institute of Physical-Chemical Medicine, Moscow.

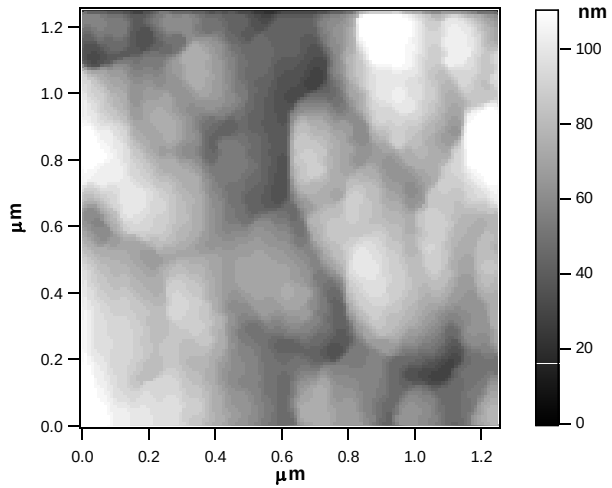

YBCO/YSZ/Ni

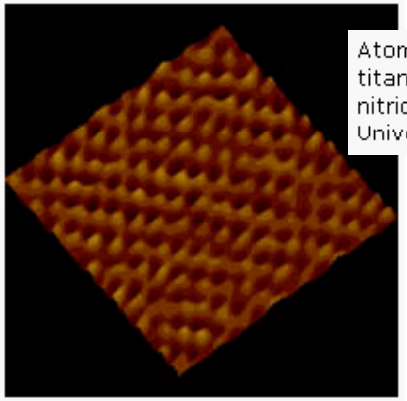

Atomic resolution image of the titanium oxide layer on top of a titanum substrate. Contact mode AFM in air, commercial silicon nitride cantalever. 5 nm scan courtesy P. Cacciafesta, University of Bristol, UK.

Atomic resolution on mica

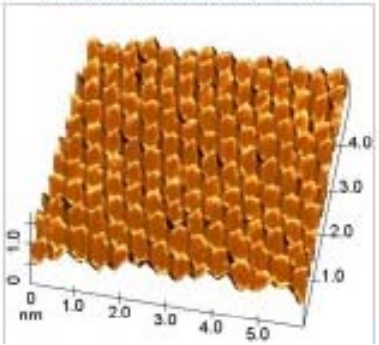

Muscovite is fairly common and is found in igneous, metamorphic and detrital sedimentary rocks. It has a layer-like structure of aluminum silicate sheets not strongly bonded, and they are held together by the K^+ ions. For further reading on this topic see the following publication: Gelatin on Mica Surfaces, **J Phys. Chem. 94**, 4611-4617.

See http://www.veeco.com

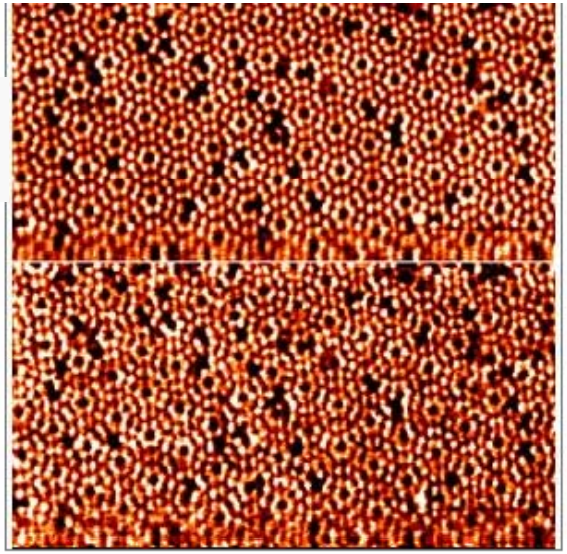

Multi-mode AFM operation : with simultaneous measurement of the topography in STM mode (upper image) with atomic resolution on Si(111)7x7 using a conductive cantilever, and of the atomic scale variation of the force, i.e. cantilever deflection (lower image).

A very few examples of AFM images II

Multi-phase systems

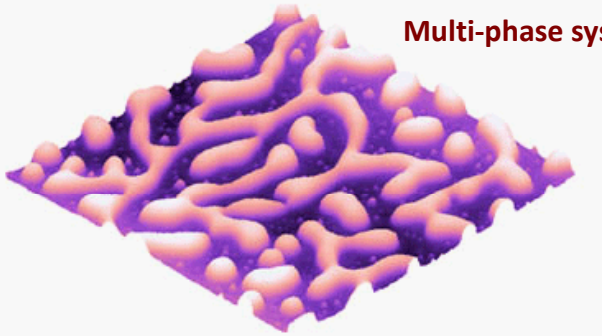

TappingMode AFM image of poly(styrene) and poly(methyl methacrylate) blend polymer film. The film was spin-cast on mica substrate from chloroform solution. The surface structure is resulted from the spinodal decomposition. The islands consist of a PMMS-rich phase while the surface matrix composes of a PS-rich phase. 3μm scan courtesy C. Ton-That, Robert Gordon University, U.K.

DNA Molecules

e high resolution of the SPM is able to discern very subtle features such as these two linear dsDNA molecules erlapping each other. 155nm scan. Image courtesy of W. Blaine Stine at email address neb@stineb.pprd.abbott.com.

A Butterfly Wing Imaged in TappingMode AFM

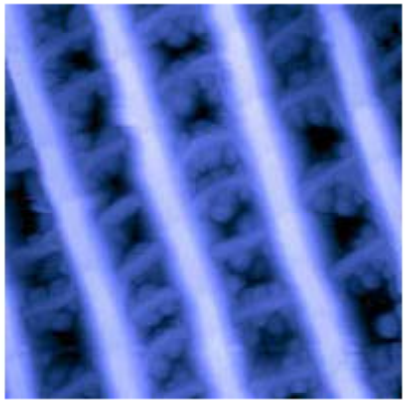

A butt... ...ered 3-D lattice is an array of holes on the cuticle of the scales. The order of such a system leads to strong diffraction of favored wavelengths in certain directions. This scattering process and pigmentation causes the coloration of the butterfly. 6.25μm scan courtesy of J. Wuest, Museum d'Histoire Naturelle, Switzerland.

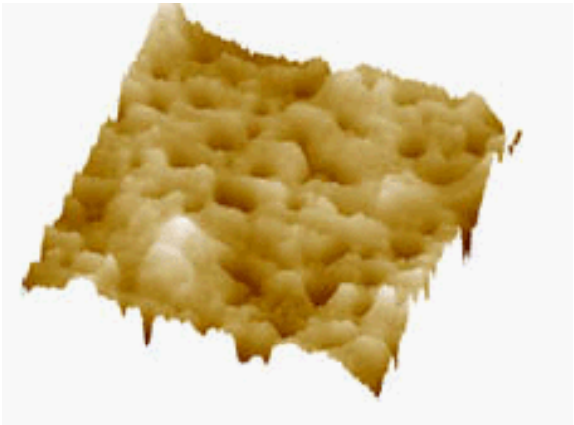

The sample is a strip of adhesive (3M Scotch tape) that has been peeled of a metal surface. The image shows small pits in the sticky surfaces of the adhesive. The image was acquired in TappingMode at frequency of 3 Hz and setpoint of 1.8 V. 2μm scan courtesy L. Scudiero, Washington State University, USA.

Huge variety of AFM applications!!

A very few examples of AFM images III

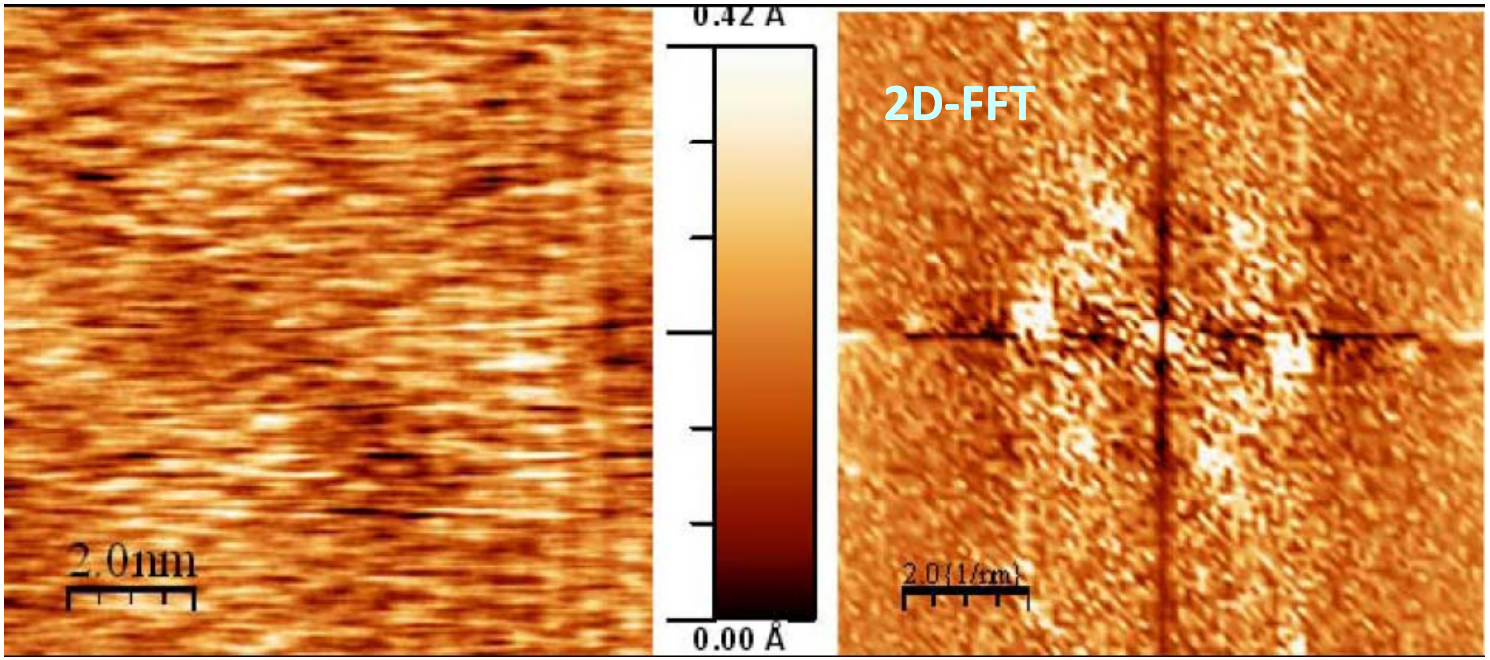

Contact-mode topography of nonanethiol SAM grown on Au/mica

Hexagonal arrangement → structural variant

$$c\left(\sqrt{3}x\sqrt{3}\right)R30°$$

Conclusions

- ✓ Invention of scanning probe microscopies (born with SM in mid ‘80s) gave impulse to analysis at the small and ultra-small scales
- ✓ Mechanical forces are at the basis of the AFM operation
- ✓ In AFM the probed quantity is the local attractive/repulsive forces
- ✓ Many variants have been introduced, remarkably the non-contact (or tapping) AFM for “soft” materials
- ✓ *(to be discussed: how AFM can measure mechanica properties at the small and ultra-small scales)*